COMMUN. MATH. SCI.
Vol. 22, No. 1, pp. 67–94

EPIDEMIC DYNAMICS AND WEALTH INEQUALITY UNDER TWO FEEDBACK CONTROL STRATEGIES*

LINGLING WANG† AND CHONG LAI‡

Abstract. A multi-agent wealth exchange model, which considers a varying trading propensity and a control of wealth inequality, is adopted to investigate the wealth distribution under infectious disease. Using the feedback control method, two saturated nonlinear incidence rates are obtained to explore the impact of the government contact control measures on epidemic dynamics and wealth distribution. We find that the contact control measures may reduce the peak of the infected fraction and make more people remain uninfected, but prolong the duration of the epidemic and increase wealth inequality. In a closed (an open) economy, the large-time behavior of wealth distribution presents a Pareto tail, and examples of trading propensity depending on wealth suggest that an increase in the savings of the wealthy may increase wealth inequality. In addition, our simulation results illustrate that the government's tax and redistribution measures can alleviate the wealth inequality caused by the contact control and improve the wealth of agents at low and middle levels.

Keywords. Wealth distribution; infectious disease; dynamic equations; feedback controls; nonlinear incidence rate.

AMS subject classifications. 35Q20; 35Q84; 35Q93; 91B80.

1. Introduction

The spread of an epidemic has a negative impact on personal lives and socio-economic development [18]. Mathematical models are employed to study the epidemic dynamics, and the relationship between the potential cost and benefit of various pandemic interventions [21, 43], which help the government to take appropriate epidemic prevention and economic control measures in time. In epidemiology, the rapid outbreaks of infectious diseases are described by compartment models, in which compartments with labels M(passively immune), S(susceptible), E(exposed), I(infective), and R(recovered) represent epidemiological classes, and the choice of compartments in epidemiology models depends on the characteristics of a particular disease [26].

In recent years, many works employ the theory of rarefied gas dynamics to study social and economic phenomena (opinion formation, wealth distribution, etc. [4, 7, 9, 13, 22–24, 38, 40]). The basic idea is that each agent is regarded as a rarefied gas molecule, and the interaction of traits (such as opinion, wealth, contact number [16], etc.) between agents is similar to collisions of molecules. To investigate the socio-economic impact of epidemics, scholars combine the epidemiological models (see [25–27]) with the social-economic phenomena of multi-agent systems by using the theory of rarefied gas dynamics [15–17], in which the trait distributions of the agent groups (such as the susceptible, infected, and recovered group) are described by Boltzmann-type equations. The trait interactions between agents with the same or different infection status, and the changes in agents' infection status, are included in the dynamic model. Dimarco et al. [16] combine the Susceptible-Infective-Recovered(SIR) model with a population-based contact dynamical model to discuss the influence of sociality on the spread of

*Received: September 02, 2022; Accepted (in revised form): May 06, 2023. Communicated by Lorenzo Pareschi.

†School of Mathematics, Southwestern University of Finance and Economics, Chengdu 611130, P.R. China (linglingw@smail.swufe.edu.cn).

‡Corresponding author. Business School, Chengdu University of Technology, Chengdu 610059, P.R. China (laichong@cdut.edu.cn).

infectious diseases, and find that the spread of infectious diseases depends on moments of the contact distribution.

Our study is related to the work in [15], in which the SIR dynamical model with the wealth exchange Cordier-Pareschi-Toscani(CPT) model in [10] are integrated together to investigate the impact of infectious diseases on wealth distribution. The research of Dimarco et al. [15] is based on the framework of the classical SIR model, in which the average number of contacts is independent of the epidemic's severity, and assumes that the wealth exchange behavior between agents follows a binary interaction rule with constant trading propensity. One contribution of this paper is that we extend the work in [15] and consider two practical factors: epidemic control and economic regulation. Our motivation is that the epidemic and economic measures taken by the government have non-negligible influences on wealth distribution and social equality [18]. In practice, before the advent and popularization of vaccines, governments took intervention measures to avoid the deterioration of the epidemic, such as developing vaccines, blocking areas with a serious epidemic, requiring people to reduce social activities, etc. Meanwhile, in response to the reduction of the labor force caused by the spread of the epidemic and the high social and economic costs of contact interventions [28], the government may take economic measures to alleviate the wealth inequality. In this paper, we investigate the impact of government contact and economic control measures on wealth distribution, and find an optimal contact control strategy to curb the epidemic and minimize economic losses.

In epidemiological models, the contact rate, which is the average number of adequate contacts per person per unit time [26], has an impact on the threshold quantity (the basic reproduction number) and the incidence rate of epidemiological models. In early infectious disease models, Hethcote [25], Kermack and McKendrick [29] assume that the agents' contact rate ρ_0 is a constant. In recent years, the contact rate is considered as a function of agents' trait (e.g., age, commuting [5,6,8]) to discuss the influence of social structure on epidemics. Before the popularization of vaccines, the government usually took non-pharmaceutical measures, such as isolation, blockade, and safe distance, to control the spread of the epidemic disease and prevent the limited health care system from being overburdened. The essence of these non-pharmaceutical measures is to reduce people's social contacts. Therefore, the impact of non-pharmaceutical measures on the transmission of the disease is mainly reflected in the adjustment of the contact rate [31,37].

Recently, with the outbreak of the COVID-19 epidemic, many works are dedicated to simulating the non-pharmaceutical containment measures. Based on the micro-updated model of the number of social contacts in [16], Dimarco et al. [17] introduce a control term to indicate the selective restriction of social activities to curb the epidemic. Using a SIR model with a social structure, Albi et al. [6] simulate the government's strategy of taking non-pharmacological interventions to reduce the spread of epidemics through an optimal control problem. Utilizing an age-dependent Susceptible-Exposed-Infectious-Recovered-Dead(SEIRD) compartment model, Albi et al. [5] consider a multiple optimal control problem depending on specific social activities (such as home, work, school, etc.), and evaluate the impact of selective relaxation of containment measures. The objective of the non-pharmacological intervention in the optimal control problem in [37] is to minimize the mortality associated with the epidemic, and it does not consider the impact of the agent's social characteristics on the epidemic. The control terms obtained from the optimal control problem in [5,6,37] are used to appropriately reduce the contact rate in the epidemic model to characterize the non-drug intervention.

In [15], the contact rate $\rho(w,v)$ is a function of two exchangers' wealth (w,v), but is not affected by the spread of disease. Inspired by the influenza pandemic model with controls in [31], in which a control term is used to model the effect of the external isolation control, we introduce a control term u_{soc} to depict the intensity of the contact control measures taken by the government to curb the epidemic, and couple the contact rate $\rho(w,v)$ with the control term u_{soc}. The time-dependent control term u_{soc} in this paper is derived from an optimal control problem by the feedback control method in [5]. Our optimal control problem simulates the government's intervention strategy with the goal to minimize the spread of virus, namely, reducing the number of infected individuals. Cost functions adopted in our work are the generalized form of perception functions in [5]. The nonlinear incidence rate $\mathcal{F}(\cdot)$ (i.e., the average number of new infected persons per unit time [32]) associated with the new cost function is verified to satisfy the biologically feasible conditions in [30] and the saturating effect in [32]. Mathematically, the incidence rate $\mathcal{F}(\cdot)$ is non-decreasing for the susceptible fraction and the infected fraction, and is a concave function of the infected fraction. Simulating and analyzing the dynamics of the contact control SIR model corresponding to the cost functions under different parameters, we obtain a new contact control strategy. The strategy is epidemic dependent, time-varying, and performs well in controlling the epidemic and minimizing economic losses.

Optimal control strategies are also employed in the research of social and economic dynamics, such as tumor growth, opinion formation, wealth distribution, etc. [1,3,12,39]. Blockade measures reduce social contacts and economic activities, alleviating the risk of virus transmission, but may also cause economic issues. The extended classical SIR model in [20] illustrates that the epidemic leads to economic recessions. Therefore, to avoid the aggravation of the wealth inequality caused by the epidemic, the government should take wealth control measures to mitigate the losses suffered by families and enterprises [20]. In a homogeneous market with multi-agents, Düring et al. [12] investigate the influence of optimal control strategy on wealth distribution, where each agents' wealth evolves according to

$$\dot{w_i}(t) = \frac{1}{N}\sum_{j=1}^{N} P_{ij}(w_j - w_i) + u_i, \qquad w_i|_{t=0} = w_{i,0} \geq 0. \tag{1.1}$$

$\dot{w_i}(t)$ is the derivative of wealth w_i of agent i about time t. The initial wealth $w_{i,0}$ of each agent is nonnegative, and the constant parameter $P_{ij} \in [0,1)$ is a measure of the exchange proportion between agent i and j $(i,j = 1,2,...,N)$. Each control u_i is achieved by minimizing the functional

$$u = \arg\min_{u\in\mathcal{U}} \frac{1}{2}\int_0^T \Big(\frac{1}{N^2}\sum_{i,j=1}^{N}|w_i - w_j|^2 + \frac{\nu}{N}\sum_{i=1}^{N}|u_i|^2\Big)dt,$$

where $u = (u_1,...,u_N)$. $\nu > 0$ is a penalization parameter, $\mathcal{U}$ is the controls' constraint space. Düring et al. [12] point out that the control term u_i in the wealth exchange model (1.1) depicts the taxation and redistribution strategy via an alternative theoretical method, and illustrate that the control affects the Pareto index of the steady-state wealth distribution.

In the study of wealth distribution, the interaction rule between agents is described by a micro wealth exchange model, one of whose typical characteristics is the exchange propensity of agents. In the Cordier-Pareschi-Toscani(CPT) model [10,33], the exchange

propensity is a non-negative constant, namely, all agents in the system have the same exchange propensity. Düring and Toscani [14] generalize the CPT model to describe the wealth exchange between different countries or different social groups within a country, in which agents have different exchange propensities. Considering that the distribution of wealth is affected by individual characteristics, the exchange propensity in [36] depends on the agent's knowledge. The results in [36] show that knowledge may enlarge wealth inequality.

The micro multi-agent wealth exchange model with feedback control used in our work is a generalization of (1.1). We think that agents are risk conscious, only part of their wealth is used for market exchange and the rest for savings. We introduce a saving propensity parameter into (1.1) to reflect the maximum proportion of personal wealth that agents are willing to exchange in the market, depending on the infection status of the agent. Assuming that agents' trading behavior is affected by their status (health status and subjective consciousness), we generalize the constant exchange propensity P_{ij} in (1.1) to functions of the infection status and wealth of both traders. In addition, the cost function in our optimal control problem is set as a weighted sum of the square of the wealth gap between agents and the square of the distance between individual wealth and the average wealth, aiming to reduce wealth inequality. Compared with the CPT model in [15], our multi-agent wealth exchange model contains more information, which may help us to analyze the impact of government and agents' decisions on wealth distribution if the epidemic occurs. An interesting finding is that, in contrast to the steady-state wealth distribution in [15], where the Pareto index depends on the ratio of agents' trading propensity to market risk, the Pareto index obtained in our work also depends on the susceptible fraction.

Assuming that the number of agents N is relatively large, we adopt the model predictive control method [2] to solve our optimal control problems. By using an appropriate quasi-invariant limits approximation [22], the Boltzmann-type equations are transformed into a Fokker-Planck system, which has an explicit steady-state solution in special cases. Using the steady-state solution of the Fokker-Planck system, we discuss the large-time behavior about wealth distribution in a closed economy when trading propensity depends on the wealth of both traders through examples, and analyze the effect of contact control measures on wealth inequality in a closed (an open) economy.

The rest of the paper is structured as follows. In Section 2, a multi-agent wealth exchange model with feedback control is introduced and a binary wealth exchange model with market risk is derived, which is the interaction rule of the collision operator in the Boltzmann-type equations. In Section 3, using the feedback control method, the government's contact control strategy is embedded in the dynamic wealth distribution model under an epidemic. The SIR epidemic model with feedback control is obtained and compared with the classical SIR model to verify the effectiveness of contact control measures in epidemic containment. Section 4 presents a Fokker-Planck asymptotic analysis of the wealth dynamics in the controlled epidemiologic model, and analyzes the influences of several parameters (agents' trading propensity, the government's control measures for the epidemic, etc.) on the large-time behavior of the wealth distribution. Section 5 numerically simulates epidemic dynamics and steady-state wealth distribution under different contact control measures, and analyzes the impact of government contact control and economic control measures (such as taxation and redistribution) on wealth distribution. Conclusions are drawn in Section 6.

2. Micro description of wealth dynamics

2.1. Multi-agent wealth exchange with feedback control. In this section, we consider a general form of the wealth exchange model (1.1). Different from the interaction between agents in one class [12], we consider three types of agents, which are classified as susceptible, infected, and recovered according to their infection status. The wealth exchange problem between agents is similar to the physical problem of mixed rarefied gas [11,14]. To reflect the differences between agents, we extend the constant exchange propensity in (1.1) as a function of traders' wealth and infection status, and assume that only parts of the agents' wealth is used for market exchange.

We suppose that each agent's state is entirely described by the infection status and the agent's wealth, meaning that agents are indistinguishable [36,41]. Here, we assume that there are no debts in the interaction. Hence, the wealth $w_i = w_i(t) \geq 0$ of agent $i \in \{1,...,N\}$ evolves as

$$\begin{aligned} \dot{w}_i &= \frac{1}{N}\sum_{j=1}^{N} P(w_i,h_i;w_j,h_j)(\gamma_j w_j - \gamma_i w_i) + \theta(1-\gamma_i)w_i + u_i, \\ w_i(t=0) &= w_{i,0} \geq 0, \end{aligned} \tag{2.1}$$

where $h_i \in \{S,I,R\}$ represents the infection status of agent i, N is the total number of agents in the wealth exchange system. The trading propensity $P(w_i,h_i;w_j,h_j) \in [0,1]$ of agent j to agent i depends on the wealth and infection status of exchangers. We assume that agents are rational and always retain certain wealth for survival. Each agent i only uses part of the personal wealth to participate in market transactions, which is expressed by a constant parameter $\gamma_i \in [0,1]$, and the rest is used for savings with interest rate θ. Compared with the wealth exchange model in [15], we take into account the redistribution effect of the government's economic strategy on wealth, which is designed to narrow the wealth gap, and use a control term $u_i = u_i(t)$ to express it. The control term $u_i = u_i(t)$ belongs to an admissible set $\mathcal{U}$ and is given by

$$u = \arg\min_{u\in\mathcal{U}} \frac{1}{2N}\int_0^T \sum_{j=1}^{N}\left[\frac{\mu_1}{N}\sum_{k=1}^{N}(w_j - w_k)^2 + \mu_2(w_j - \bar{w})^2 + \nu|u_j|^2\right]dt, \tag{2.2}$$

where $u = (u_1,...,u_N)$, constants $\mu_1 \geq 0$ and $\mu_2 \geq 0$ satisfy $\mu_1 + \mu_2 = 1$. The penalty parameter $\nu > 0$ indicates the importance of control u (see [3]). In (2.2), the target cost functional $L := \sum_{j=1}^{N}\left[\sum_{k=1}^{N}\mu_1(w_j - w_k)^2/N + \mu_2(w_j - \bar{w})^2\right]$ measures the degree of wealth inequality, and $\bar{w}$ is the average wealth.

The method of model predictive control [1,3,12,42] (receding horizon strategy or instantaneous control in engineering [34]) is employed to solve the optimal control problem (2.1) and (2.2). Let $[0,T] = \bigcup_{n=0}^{N_T-1}[t^n,t^{n+1}]$, where $t^0 = 0$, $t^{N_T} = T$ and $t^{n+1} - t^n := \Delta t$. Using Euler discretization method, we transform the wealth exchange Equation (2.1) on $[0,T]$ into discrete equations. Then the control problem is solved in each small time interval $[t^n,t^{n+1}]$ and

$$w_i^{n+1} = w_i^n + \frac{\Delta t}{N}\sum_{j=1}^{N} P_{ij}^n(\gamma_j w_j^n - \gamma_i w_i^n) + \theta(1-\gamma_i)w_i^n\Delta t + \Delta t u_i^n, \tag{2.3}$$

$$u_i^n = \arg\min_{u_i\in\mathcal{U}} \frac{1}{2N}\sum_{j=1}^{N}\left[\frac{\mu_1}{N}\sum_{k=1}^{N}(w_j^{n+1} - w_k^{n+1})^2 + \mu_2(w_j^{n+1} - \bar{w}^{n+1})^2 + \nu|u_j^n|^2\right], \tag{2.4}$$

where $P_{ij}^n := P(w_i^n, h_i^n; w_j^n, h_j^n)$ and $\bar{w}^{n+1} = \sum_{i=1}^{N} w_i^{n+1}/N$. w_i^n, h_i^n and u_i^n represent the values of variables w_i, h_i and u_i at time t^n, respectively.

Employing the Lagrange multiplier method, the instantaneous feedback control term u_i^n is deduced from the control problems (2.3) and (2.4) in the form

$$u_i^n = -\frac{(1+\mu_1)\Delta t}{\nu}(w_i^{n+1} - \bar{w}^{n+1}). \tag{2.5}$$

Equation (2.5) leads to $\sum_{i=1}^{N} u_i^n \equiv 0$, meaning that all taxes are redistributed among agents. Therefore, from (2.3), we have the relationship

$$\bar{w}^{n+1} = \bar{w}^n + \frac{\Delta t}{N^2}\sum_{i,j=1}^{N} P_{ij}^n(\gamma_j w_j^n - \gamma_i w_i^n) + \frac{\theta\Delta t}{N}\sum_{j=1}^{N}(1-\gamma_j)w_j^n. \tag{2.6}$$

Substituting (2.3) and (2.6) into (2.5), the explicit expression of the control term u_i^n reads

$$\begin{aligned} u_i^n = -\frac{(1+\mu_1)\Delta t}{\nu+(1+\mu_1)\Delta^2 t}\Bigg[& w_i^n - \bar{w}^n + \frac{\Delta t}{N}\sum_{j=1}^{N} P_{ij}^n(\gamma_j w_j^n - \gamma_i w_i^n) \\ & + \theta(1-\gamma_i)w_i^n\Delta t - \frac{\Delta t}{N^2}\sum_{i,j=1}^{N} P_{ij}^n(\gamma_j w_j^n - \gamma_i w_i^n) - \frac{\theta\Delta t}{N}\sum_{j=1}^{N}(1-\gamma_j)w_j^n\Bigg]. \end{aligned} \tag{2.7}$$

2.2. Binary wealth exchange with control and risk. Based on the multi-agents wealth exchange model in Section 2.1, we study the interaction between two agents, namely, $N=2$. From (2.3) and (2.7), the binary wealth exchange model is derived in the form

$$\begin{aligned} w_i^{n+1} = \big[1+2\theta\alpha(1-\gamma_i)\big]w_i^n + \alpha\big[P_{ij}^n - \beta(P_{ij}^n + P_{ji}^n) - 2\theta\beta\big](\gamma_j w_j^n - \gamma_i w_i^n) \\ -\beta(1+2\theta\alpha)(w_i^n - w_j^n), \end{aligned} \tag{2.8}$$

where $\alpha = \Delta t/2$, $\beta = \Delta t/(2(\gamma+\Delta t))$ and $\nu = 2(1+\mu_1)\gamma\alpha$.

Let (w,v) represent the pre-trade wealth of two agents with infection status $H \in \{S,I,R\}$ and $\Lambda \in \{S,I,R\}$, respectively, and (w^*,v^*) denote their post-trade wealth. Assuming that agents with the same infection status have a common saving propensity, and their infection status remains unchanged in a single interaction. According to (2.8) and taking into account the influence of risks, the microscope binary wealth exchange model is given by

$$w^* = [1+2\theta\alpha(1-\gamma_H)]w - \beta(1+2\theta\alpha)(w-v) + [T_{H\Lambda}(w,v) - 2\theta\alpha\beta](\gamma_\Lambda v - \gamma_H w) + \eta_1 w, \tag{2.9a}$$

$$v^* = [1+2\theta\alpha(1-\gamma_\Lambda)]v - \beta(1+2\theta\alpha)(v-w) + [T_{\Lambda H}(v,w) - 2\theta\alpha\beta](\gamma_H w - \gamma_\Lambda v) + \eta_2 v, \tag{2.9b}$$

where

$$\begin{aligned} T_{H\Lambda}(w,v) &= \alpha P(w,H;v,\Lambda) - \alpha\beta[P(v,\Lambda;w,H) + P(w,H;v,\Lambda)], \\ T_{\Lambda H}(v,w) &= \alpha P(v,\Lambda;w,H) - \alpha\beta[P(v,\Lambda;w,H) + P(w,H;v,\Lambda)]. \end{aligned}$$

The random variables η_1 and η_2 represent market risks, and their diffusion intensity are related to the agent's wealth. Suppose that the random variables η_1 and η_2 are independent and identically distributed with mean zero and variance σ^2.

REMARK 2.1. To ensure the non-negativity of post-trade wealth w^*, v^*, it is necessary to assume

$$\eta_1 \geq \beta + \alpha\gamma_H - 1, \qquad \eta_2 \geq \beta + \alpha\gamma_\Lambda - 1$$

for every fixed $\alpha \leq 1$.

In fact, (2.9a) is rewritten as

$$\begin{aligned} w^* = &\Big[1-\beta-\gamma_H T_{H\Lambda}(w,v) + 2\theta\alpha(1-\beta)(1-\gamma_H) + \eta_1\Big] w \\ &+ \Big[\beta + \gamma_\Lambda T_{H\Lambda}(w,v) + 2\theta\alpha\beta(1-\gamma_\Lambda)\Big] v. \end{aligned}$$

Using $\beta = \Delta t/(2(\gamma+\Delta t)) < 1/2$, we have

$$\beta + \gamma_\Lambda T_{H\Lambda}(w,v) + 2\theta\alpha\beta(1-\gamma_\Lambda) \geq \beta(1-\alpha\gamma_\Lambda) + \alpha(1-\beta)P(w,H;v,\Lambda)\gamma_\Lambda > 0$$

and

$$\beta + \gamma_H T_{H\Lambda}(w,v) - 2\theta\alpha(1-\beta)(1-\gamma_H) \leq \beta + \alpha\gamma_H \leq 1. \tag{2.10}$$

From (2.10), the restrictive condition $\eta_1 \geq \beta + \alpha\gamma_H - 1$ is sufficient to guarantee that the post-trade wealth $w^* \geq 0$.

From the binary interaction (2.9), we have

$$\begin{aligned} \langle w^* + v^* \rangle = w + v + &\alpha\Big[\gamma_H(P(v,\Lambda;w,H) - P(w,H;v,\Lambda)) + 2\theta(1-\gamma_H)\Big] w \\ &+ \alpha\Big[\gamma_\Lambda(P(w,H;v,\Lambda) - P(v,\Lambda;w,H)) + 2\theta(1-\gamma_\Lambda)\Big] v, \end{aligned}$$

where $\langle\cdot\rangle$ is the mathematical expectation in terms of η_1 and η_2. In particular, if trading propensities $P(w,H;v,\Lambda)$ and $P(v,\Lambda;w,H)$ satisfy

$$\big[P(w,H;v,\Lambda) - P(v,\Lambda;w,H)\big](\gamma_H w - \gamma_\Lambda v) = 2\theta\big[(1-\gamma_H)w + (1-\gamma_\Lambda)v\big], \tag{2.11}$$

the wealth of the binary interaction system is conserved in statistic, i.e $\langle v^* + w^* \rangle = v + w$.

3. Wealth dynamics in a controlled SIR epidemiologic model

Similar to the classical SIR model in [25–27], agents are divided into three groups: susceptible, infected, and recovered. The susceptible group refers to the individuals who have no immunity and may be infected with the disease, the infected group includes those who are infectious and can transmit the disease, and the recovered group consists of those who are healed or with permanent immunity.

Let $f_\Lambda(w,t)$ represent the wealth distribution of agents in class $\Lambda \in \{S, I, R\}$ at $t \geq 0$. The change of wealth distributions in the background of the epidemic are due to two aspects [15]. On one hand, in the course of a market transaction, an agent may change from one health status to another due to exposure to an infected virus or medical treatment. On the other hand, binary trading activities lead to changes between gain

and loss of the agents' wealth [14]. Then, the time evolution of $f_\Lambda(w,t)$, $\Lambda\in\{S,I,R\}$ is written as a coupling form of transport and collision process, namely,

$$\frac{\partial f_S(w,t)}{\partial t} = -\Xi(w,t)f_S(w,t) + \sum_{\Lambda\in\{S,I,R\}} Q(f_S,f_\Lambda)(w,t), \tag{3.1a}$$

$$\frac{\partial f_I(w,t)}{\partial t} = \Xi(w,t)f_S(w,t) - r(w)f_I(w,t) + \sum_{\Lambda\in\{S,I,R\}} Q(f_I,f_\Lambda)(w,t), \tag{3.1b}$$

$$\frac{\partial f_R(w,t)}{\partial t} = r(w)f_I(w,t) + \sum_{\Lambda\in\{S,I,R\}} Q(f_R,f_\Lambda)(w,t), \tag{3.1c}$$

where $r(w)$ is the recovery rate, $\Xi(w,t)$ is the rate of susceptible individuals transforming into infected individuals.

For any test function $\psi(w)\in C_0^\infty(\mathbb{R}_+)$, the weak form of (3.1) is

$$\begin{aligned}\frac{d}{dt}\int_{\mathbb{R}_+} f_S(w,t)\psi(w)dw = &-\int_{\mathbb{R}_+}\Xi(w,t)f_S(w,t)\psi(w)dw\\ &+\sum_{\Lambda\in\{S,I,R\}}\int_{\mathbb{R}_+} Q(f_S,f_\Lambda)(w,t)\psi(w)dw,\end{aligned} \tag{3.2a}$$

$$\begin{aligned}\frac{d}{dt}\int_{\mathbb{R}_+} f_I(w,t)\psi(w)dw = &\int_{\mathbb{R}_+}\Xi(w,t)f_S(w,t)\psi(w)dw - \int_{\mathbb{R}_+} r(w)f_I(w,t)\psi(w)dw\\ &+\sum_{\Lambda\in\{S,I,R\}}\int_{\mathbb{R}_+} Q(f_I,f_\Lambda)(w,t)\psi(w)dw,\end{aligned} \tag{3.2b}$$

$$\begin{aligned}\frac{d}{dt}\int_{\mathbb{R}_+} f_R(w,t)\psi(w)dw = &\int_{\mathbb{R}_+} r(w)f_I(w,t)\psi(w)dw\\ &+\sum_{\Lambda\in\{S,I,R\}}\int_{\mathbb{R}_+} Q(f_R,f_\Lambda)(w,t)\psi(w)dw.\end{aligned} \tag{3.2c}$$

Specifically, the weak form of the Boltzmann-type collision operator $Q(\cdot,\cdot)$ is expressed as

$$\begin{aligned}&\int_{\mathbb{R}_+} Q(f_H,f_\Lambda)(w,t)\psi(w)dw\\ =&\left\langle\int_{\mathbb{R}_+^2} B_{H\Lambda}\cdot\big(\psi(w^*)-\psi(w)\big)f_H(w,t)f_\Lambda(v,t)dvdw\right\rangle,\quad H,\Lambda\in\{S,I,R\}.\end{aligned} \tag{3.3}$$

The non-negative interaction kernel $B_{H\Lambda}$, which is related to the probability of microscopic interaction between agents of classes H and Λ, is considered as

$$B_{H\Lambda} = c_{H\Lambda}\cdot\chi(w^*\geq 0)\cdot\chi(v^*\geq 0). \tag{3.4}$$

The constant $c_{H\Lambda}>0$ represents the interaction frequency of agents for classes H and Λ, and $\chi(\cdot)$ is the indicator function. The interaction kernel (3.4) with suitable $c_{H\Lambda}$ guarantees that the post-trade wealth is non-negative.

3.1. SIR epidemic model with contact control. Considering the implementation of government contact control measures, the transformation rate $\Xi(w,t)$ in (3.1)

is expressed as

$$\Xi(w,t)=\int_{\mathbb{R}_+}\rho(w,v)[1-\lambda u_{soc}(t)]f_I(v,t)dv, \tag{3.5}$$

where $\rho(w,v)$ is the contact rate between two agents with wealth w and v without isolation measures. The control term $u_{soc}(t)\in[0,1]$ represents the government's efforts to reduce contact between agents to prevent the spread of virus, and the constant $\lambda\in[0,1]$ measures the effectiveness of the control strategy's application.

Let $S(t)$, $I(t)$ and $R(t)$ represent the fraction of agents in the susceptible, infected and recovered class, respectively. We have $H(t)=\int_{\mathbb{R}_+}f_H(w,t)dw$, $H\in\{S,I,R\}$. We introduce an objective functional $\mathcal{J}$ to determine the government's strategy, so as to reduce the number of infections and the incidence rate in the time interval $[0,T]$. Then the control term $u_{soc}(t)$ is derived from the optimal control problem

$$\begin{aligned}u_{soc}(t)&=\underset{u_{soc}\in\tilde{\mathcal{U}}}{argmin}\,\mathcal{J}(u_{soc})\\&=\underset{u_{soc}\in\tilde{\mathcal{U}}}{argmin}\int_0^T\left[\Phi(S(\tilde{t}),I(\tilde{t}))+\frac{1}{2}\nu_{soc}|u_{soc}(\tilde{t})|^2\right]d\tilde{t},\end{aligned}$$

where $\Phi(\cdot)$ is a cost functional, ν_{soc} is a penalty parameter. $\tilde{\mathcal{U}}$ is an admissible set, in which the control term u_{soc} takes values to keep a monotonic decreasing trend of the number of susceptible individuals.

Similar to the wealth inequality control model in Section 2.1, the feedback control method (see [5,6]) is adopted to derive the social contact control term u_{soc}. We have

$$u_{soc}(t)=\underset{u_{soc}\in\tilde{\mathcal{U}}}{argmin}\left\{\Phi(S(t),I(t+\Delta t))+\frac{1}{2}\nu_{soc}|u_{soc}(t)|^2\right\}. \tag{3.6}$$

Substituting $\psi(w)=1$ into (3.2), we get the evolution process of the fractions $S(t)$, $I(t)$ and $R(t)$.

$$\frac{dS(t)}{dt}=-\int_{\mathbb{R}_+^2}\rho(w,v)[1-\lambda u_{soc}(t)]f_S(w,t)f_I(v,t)dvdw, \tag{3.7a}$$

$$\frac{dI(t)}{dt}=\int_{\mathbb{R}_+^2}\rho(w,v)[1-\lambda u_{soc}(t)]f_S(w,t)f_I(v,t)dvdw-\int_{\mathbb{R}_+}r(v)f_I(v,t)dv, \tag{3.7b}$$

$$\frac{dR(t)}{dt}=\int_{\mathbb{R}_+}r(v)f_I(v,t)dv. \tag{3.7c}$$

Discretizing (3.7b) with respect to time, then the infected fraction at time $t+\Delta t$ is given by

$$\begin{aligned}I(t+\Delta t)=I(t)&+\Delta t\int_{\mathbb{R}_+^2}\rho(w,v)[1-\lambda u_{soc}(t)]f_S(w,t)f_I(v,t)dvdw\\&-\Delta t\int_{\mathbb{R}_+}r(v)f_I(v,t)dv.\end{aligned} \tag{3.8}$$

Differentiate the objective functional in (3.6) about the control variable u_{soc}, and combine with (3.8) to obtain the control term

$$u_{soc}(t)=\frac{\lambda}{\kappa}\frac{\partial\Phi}{\partial I}\cdot\int_{\mathbb{R}_+^2}\rho(w,v)f_S(w,t)f_I(v,t)dvdw, \tag{3.9}$$

where $\nu_{soc}=\kappa\Delta t$. In the case of $\lambda=0$ or $\kappa=\infty$, the control item $u_{soc}(t)$ is zero and the transformation rate (3.5) becomes that in [15].

PROPOSITION 3.1. *Assuming that the contact rate $\rho(w,v)=\rho$ and the recovery rate $r(w)=r$ are constant, and let $(S(t),I(t))$ be a solution of (3.7) in*

$$\left\{(S(t),I(t))\middle| S(t)\geq 0, I(t)\geq 0, S(t)+I(t)+R(t)=1\right\}.$$

Then the steady-state solutions $S^\infty=\lim_{t\to\infty}S(t)$ and $R^\infty=\lim_{t\to\infty}R(t)$ exist. The infected fraction $I(t)$ in the steady state $(t\to\infty)$ tends to zero.

Proof. From (3.7), the susceptible fraction $S(t)$ decreases with time t and has a lower bound 0, the recovered fraction $R(t)$ increases with time and has an upper bound 1. By the monotone bounded convergence theorem, the limitation $S^\infty=S(t=\infty)$ and $R^\infty=R(t=\infty)$ exist.

From (3.7b), we have

$$\frac{dI(t)}{dt}\leq[\rho S(t)-r]I(t).$$

If the proportion of susceptible agents at the initial time satisfies $S_0<r/\rho$, then the infected fraction $I(t)$ decreases monotonically to zero.

In the case of $S_0>r/\rho$, if $I^\infty\neq 0$, then $dR/dt>0$ and $R^\infty=\infty$, which contradicts $R^\infty\leq 1$. Therefore, the infected fraction $I(t)$ in the steady state tends to zero. ∎

PROPOSITION 3.2. *Let $\rho(w,v)\leq\rho_0$ and $\partial\Phi/\partial I\geq 0$ be monotonic about the infected fraction I. Then for all times $t>0$, solutions to (3.7) are admissible if the penalty parameter κ satisfies*

$$\kappa>\lambda^2\rho_0 S_0 I_{max}\left.\frac{\partial\Phi}{\partial I}\right|_{I=I^*}, \tag{3.10}$$

where

$$I^*=\begin{cases}0, & \text{if } \frac{\partial^2\Phi}{\partial I^2}<0,\\ I_{max}, & \text{if } \frac{\partial^2\Phi}{\partial I^2}>0.\end{cases}$$

I_{max} is the peak of the proportion of the infected.

Proof. To maintain the monotonically decreasing trend of the number of susceptible individuals, $\lambda u_{soc}(t)<1$ is required in (3.5). Therefore, from (3.9), for any time $t>0$, we will prove the inequality

$$\lambda^2\frac{\partial\Phi}{\partial I}\cdot\int_{\mathbb{R}_+^2}\rho(w,v)f_S(w,t)f_I(v,t)dvdw<\kappa. \tag{3.11}$$

According to Proposition 3.1, the infected fraction in the steady state is 0. Therefore, when $\partial^2\Phi/\partial I^2<0$, $\partial\Phi/\partial I$ reaches the maximum at $I^*=0$. When $\partial^2\Phi/\partial I^2>0$, $\partial\Phi/\partial I$ reaches the maximum value at $I^*=I_{max}$. In addition, the susceptible fraction $S(t)$ decreases with time t. Then $S_0\geq S(t)$ for all times $t\geq 0$. Thus, (3.10) is a sufficient condition to guarantee that inequality (3.11) holds. ∎

For the feedback control SIR model (3.7), when the contact rate $\rho(w,v)=\rho$ and the recovery rate $r(w)=r$ are constants, and $\lambda=0$ or $\kappa=\infty$, it becomes the classical SIR model [27]

$$\frac{dS(t)}{dt}=-\rho S(t)I(t), \tag{3.12a}$$

$$\frac{dI(t)}{dt}=\rho S(t)I(t)-rI(t), \tag{3.12b}$$

$$\frac{dR(t)}{dt}=rI(t). \tag{3.12c}$$

Before comparing the relationship between quantities of epidemic dynamics (3.7) and (3.12), such as the steady-state solutions and the peak of infected fraction, we denote $\sigma_0=\rho/r$ and recall the properties of the classical SIR model (3.12).

THEOREM 3.1 ([27]). *Assume that $(S(t),I(t))$ is a solution of (3.12) in*

$$\left\{\big(S(t),I(t)\big)\,\middle|\,S(t)\geq 0,I(t)\geq 0,S(t)+I(t)\leq 1\right\}.$$

If $\sigma_0 S_0\leq 1$, then $I(t)$ decreases to zero as $t\to\infty$. If $\sigma_0 S_0>1$, then $I(t)$ first increases up to a maximum value $I_{max}=I_0+S_0-1/\sigma_0-[ln(\sigma_0 S_0)]/\sigma_0$ and then decreases to zero as $t\to\infty$. The susceptible fraction $S(t)$ is a decreasing function and the limiting value S^∞ is the unique root in $(0,1/\sigma_0]$ of the equation

$$S_0+I_0-S^\infty+\frac{1}{\sigma_0}\ln\frac{S^\infty}{S_0}=0. \tag{3.13}$$

PROPOSITION 3.3. *Suppose $\rho(w,v)=\rho$, $r(w)=r$, and the parameters of system (3.7) satisfy Proposition 3.2. Let $(S^\infty_{soc},I^\infty_{soc},R^\infty_{soc})$ and $(S^\infty_*,I^\infty_*,R^\infty_*)$ be the steady-state solutions of the system (3.7) and the classical SIR model (3.12), respectively, then*

$$S^\infty_{soc}\geq S^\infty_*,\qquad I^\infty_{soc}=I^\infty_*=0,\qquad \text{and}\qquad R^\infty_{soc}\leq R^\infty_*.$$

Proof. According to Proposition 3.1 and Theorem 3.1, the steady-state infected fraction of the system (3.7) and the classical SIR model (3.12) is 0, i.e. $I^\infty_{soc}=I^\infty_*=0$.

Divide (3.7b) by (3.7a), and integrate over $[0,\infty]$ with respect to time t to obtain

$$I^\infty-I_0=S_0-S^\infty+\int_0^\infty\frac{r}{\rho S(t)[1-\lambda u_{soc}(t)]}dS(t).$$

Since $S(t)$ decreases with time t, and $\rho[1-\lambda u_{soc}(t)]\leq\rho$ for any time t, the steady-state solution S^∞_{soc} of (3.7) satisfies the inequality

$$I_0+S_0-S^\infty_{soc}+\frac{1}{\sigma_0}\ln\frac{S^\infty_{soc}}{S_0}\geq 0.$$

Let $g(x)=I_0+S_0-x+\frac{1}{\sigma_0}\ln\frac{x}{S_0}$, which is a concave function on $[0,1]$. We observe that $g(x)$ possesses a unique maximum point $x=1/\sigma_0$, and $g(1)=0$, $\lim_{x\to 0}g(x)=-\infty$. In addition, Theorem 3.1 indicates that $S^\infty_*\in(0,1/\sigma_0)$ is a solution of $g(x)=0$. Thus, $S^\infty_{soc}\geq S^\infty_*$ and $R^\infty_{soc}\leq R^\infty_*$. ∎

Proposition 3.3 shows that compared with the classical SIR epidemic model (3.12), the contact control measures taken by the government enable more agents to stay in a healthy state.

PROPOSITION 3.4. *Suppose $\rho(w,v)=\rho$, $r(w)=r$, and the parameters of system (3.7) satisfy Proposition 3.2. Let $I_{soc}^{\max}$ and $I_{*}^{\max}$ be the peak of infected fraction of the system (3.7) and the classical SIR model (3.12), respectively, then*

$$I_{soc}^{\max} \le I_{*}^{\max}.$$

Proof. If $\rho(w,v)=\rho$, $r(w)=r$, and the parameters of system (3.7) satisfy Proposition 3.2, then (3.7b) is rewritten as

$$\frac{dI(t)}{dt} = \big[\rho\big(1-\lambda u_{soc}(t)\big)S(t) - r\big]I(t). \tag{3.14}$$

According to (3.14) and (3.9), if the parameters at the initial time satisfy the inequality $\big(1-\lambda u_{soc}(0)\big)\rho S_0 > r$, the infected fraction $I(t)$ increases with time to reach the peak $I_{soc}^{\max}$, and then decreases to the steady state $I_{soc}^{\infty}=0$.

Suppose that the classical SIR model (3.12) and the feedback control SIR model (3.7) get their infected fraction's peak at time t_* and t_{soc}, respectively. From (3.14), we have

$$S(t_{soc}) = \frac{r}{\rho\big[1-\lambda u_{soc}(t_{soc})\big]} \ge \frac{r}{\rho}.$$

Divide (3.7b) by (3.7a) and integrate on $[0,t_{soc}]$ with respect to time t to obtain

$$I_{soc}^{\max} = I_0 + S_0 - S(t_{soc}) + \int_0^{t_{soc}} \frac{r}{\rho\big(1-\lambda u_{soc}(\tau)\big)S(\tau)} dS(\tau).$$

From Theorem 3.1, for the classical SIR model (3.12), we have

$$I_{*}^{\max} = I_0 + S_0 - S(t_*) + \frac{r}{\rho}\ln\frac{S(t_*)}{S_0} \qquad \text{and} \qquad S(t_*) = \frac{r}{\rho}.$$

Thus

$$\begin{aligned} I_{soc}^{\max} - I_{*}^{\max} &= S(t_*) - S(t_{soc}) - \frac{r}{\rho}\ln\frac{S(t_*)}{S_0} + \int_0^{t_{soc}} \frac{r}{\rho\big(1-\lambda u_{soc}(\tau)\big)S(\tau)} dS(\tau) \\ &\le S(t_*) - S(t_{soc}) - \frac{r}{\rho}\ln\frac{S(t_*)}{S_0} + \frac{r}{\rho}\ln\frac{S(t_{soc})}{S_0} \\ &= \frac{r}{\rho}\left[\ln\frac{S(t_{soc})}{S(t_*)} - \frac{S(t_{soc})}{S(t_*)} + 1\right]. \end{aligned}$$

Because $f(x)=\ln x - x + 1$ is a concave function of x, and the maximum value is obtained at $x=1$, so $f(x)\le f(1)=0$. Using $\frac{S(t_{soc})}{S(t_*)} \ge 1$, we have $I_{soc}^{\max} \le I_{*}^{\max}$. ∎

REMARK 3.1. The above analysis of epidemic control can be generalized to epidemic models including more compartments, and may be subject to more complex computational derivations. Similar to (3.1), we assume that the wealth distributions in an epidemic model with Susceptible-Exposed-Infected-Asymptomatic-Recovered (SEIAR) compartments [17] evolve as

$$\frac{\partial f_S(w,t)}{\partial t} = -\tilde{\Xi}(w,t)f_S(w,t) + \sum_{\Lambda\in\Omega} Q(f_S, f_\Lambda)(w,t), \tag{3.15a}$$

$$\frac{\partial f_E(w,t)}{\partial t} = \tilde{\Xi}(w,t) f_S(w,t) - r_E f_E(w,t) + \sum_{\Lambda\in\Omega} Q(f_E, f_\Lambda)(w,t), \tag{3.15b}$$

$$\frac{\partial f_I(w,t)}{\partial t} = \zeta r_E f_E(w,t) - r_I f_I(w,t) + \sum_{\Lambda\in\Omega} Q(f_I, f_\Lambda)(w,t), \tag{3.15c}$$

$$\frac{\partial f_A(w,t)}{\partial t} = (1-\zeta) r_E f_E(w,t) - r_A f_A(w,t) + \sum_{\Lambda\in\Omega} Q(f_A, f_\Lambda)(w,t), \tag{3.15d}$$

$$\frac{\partial f_R(w,t)}{\partial t} = r_I f_I(w,t) + r_A f_A(w,t) + \sum_{\Lambda\in\Omega} Q(f_R, f_\Lambda)(w,t), \tag{3.15e}$$

where $\Omega = \{S,E,I,A,R\}$, r_I and r_A are the recovery rates of infected and asymptomatic infected individuals, respectively. $\zeta \in [0,1]$ represents the proportion of exposed people who become infected, and r_E is the rate of transition from exposed persons to infected persons. We suppose that the transformation rate of susceptible individuals into infected or asymptomatic infected individuals is

$$\tilde{\Xi}(w,t) = \int_{\mathbb{R}_+} \rho_I(w,v)[1-\lambda u_{soc,1}(t)] f_I(v,t) dv + \int_{\mathbb{R}_+} \rho_A(w,v)[1-\lambda u_{soc,2}(t)] f_A(v,t) dv,$$

where the control terms $u_{soc,1}(t)$ and $u_{soc,2}(t)$ are derived from the optimal control problem

$$\begin{aligned} &(u_{soc,1}(t), u_{soc,2}(t)) \\ &= argmin \int_0^T \left\{ \Phi(S(\tilde{t}), I(\tilde{t}), A(\tilde{t})) + \frac{1}{2} \nu_{soc} \left[|u_{soc,1}(\tilde{t})|^2 + |u_{soc,2}(\tilde{t})|^2 \right] \right\} d\tilde{t}. \end{aligned} \tag{3.16}$$

$A(t) = \int_{\mathbb{R}_+} f_A(w,t) dw$ is the asymptomatic infected fraction at time t.

When the contact rates ρ_I and ρ_A are constants, integrating (3.15) with respect to w on $\mathbb{R}_+$ yields

$$\frac{dS(t)}{dt} = -\rho_I[1-\lambda u_{soc,1}(t)] S(t) I(t) - \rho_A[1-\lambda u_{soc,2}(t)] S(t) A(t), \tag{3.17a}$$

$$\frac{dE(t)}{dt} = \rho_I[1-\lambda u_{soc,1}(t)] S(t) I(t) + \rho_A[1-\lambda u_{soc,2}(t)] S(t) A(t) - r_E E(t), \tag{3.17b}$$

$$\frac{dI(t)}{dt} = \zeta r_E E(t) - r_I I(t), \tag{3.17c}$$

$$\frac{dA(t)}{dt} = (1-\zeta) r_E E(t) - r_A A(t), \tag{3.17d}$$

$$\frac{dR(t)}{dt} = r_I I(t) + r_A A(t), \tag{3.17e}$$

where $E(t) = \int_{\mathbb{R}_+} f_E(w,t) dw$ is the exposed fraction. In the case of $\rho_A = 0$ and $\zeta = 1$, (3.17) becomes an SEIR epidemic model.

Following the feedback control method in [5] and using (3.16), the control terms in (3.17) are

$$u_{soc,1}(t) = \frac{\lambda \rho_I r_E}{\tilde{\kappa}} \left[\zeta \frac{\partial \Phi}{\partial I} + (1-\zeta) \frac{\partial \Phi}{\partial A} \right] \cdot S(t) I(t),$$

$$u_{soc,2}(t) = \frac{\lambda \rho_A r_E}{\tilde{\kappa}} \left[\zeta \frac{\partial \Phi}{\partial I} + (1-\zeta) \frac{\partial \Phi}{\partial A} \right] \cdot S(t) A(t),$$

where $\tilde{\kappa}=\nu_{soc}/(\Delta t)^2$. According to (3.17), $S(t)$ and $R(t)$ are monotonically bounded, we have $E^\infty=I^\infty=A^\infty=0$ in the steady-state.

3.2. Nonlinear incidence rates. When the contact rate $\rho(w,v)=\rho$ is a constant, from (3.7) and (3.9), the incidence rate $\mathcal{F}(S,I)$ reads

$$\mathcal{F}(S,I)=\rho\left[1-\frac{\lambda^2\rho}{\kappa}\frac{\partial\Phi}{\partial I}S(t)I(t)\right]S(t)I(t), \tag{3.18}$$

which is determined by the form of the cost functional $\Phi(S,I)$.

In model (3.12), the incidence rate $\mathcal{F}(S,I)=\rho SI$ is a bilinear function of the susceptible fraction $S(t)$ and the infected fraction $I(t)$, and excludes the saturation effect. When the infected fraction is high, agents will be exposed to the disease, so the transmission rate may respond more slowly than those to linear increase in the number of infected persons [30,32]. Next, we introduce two cost functions to derive two nonlinear incidence rates, which are examples of saturating incidence rates.

Consider two cost functionals

$$\Phi_1(S,I)=\frac{\ln(1+cI^{p_1}(t))}{p_1cS(t)},\qquad 0<p_1\le 1, c=\frac{\lambda^2\rho}{\kappa} \tag{3.19}$$

and

$$\Phi_2(S,I)=\frac{I^{p_2}(t)}{p_2S^q(t)},\qquad p_2\ge 1, 0\le q\le 1. \tag{3.20}$$

In particular, the cost functional $\Phi_1(S,I)$ with $p_1=1$ and the cost functional $\Phi_2(S,I)$ with $q=0$ are introduced in [5] to describe the policy maker's perception of the epidemic's influences.

For the cost functional (3.19), we get $\partial\Phi_1/\partial I>0$, $\partial^2\Phi_1/\partial I^2<0$ and $\Phi_1(S,I)\ge I$, so $\Phi_1(S,I)$ is an increasing concave function of the infected fraction I, overestimating the number of infected agents. From (3.20), we have $\partial\Phi_2/\partial I>0$ and $\partial^2\Phi_2/\partial I^2\ge 0$. Then $\Phi_2(S,I)$ is an increasing convex function of the infected fraction I. However, the number of infected agents is overestimated when $p_2=1$ and underestimated when $p_2\ge 2$.

Substituting cost functionals (3.19) and (3.20) into (3.18), we obtain the corresponding incidence rates

$$\mathcal{F}_1(S,I)=\frac{\rho S(t)I(t)}{1+cI^{p_1}(t)}, \tag{3.21}$$

$$\mathcal{F}_2(S,I)=\rho\left[1-cS^{1-q}(t)I^{p_2}(t)\right]S(t)I(t). \tag{3.22}$$

In particular, (3.21) is a special case of the nonlinear incidence rate $\rho I^pS/(1+\alpha I^q)$ $(p>0,q>0,\alpha>0)$ in [30]. The nonlinear incidence rate (3.22) in the case of $q=1$ is considered in [19]. Simple calculations verify that the incidence rate (3.21) and (3.22) satisfy the biologically feasible conditions [30]:

$$\mathcal{F}(0,I)=\mathcal{F}(S,0)=0$$

and

$$\frac{\partial\mathcal{F}(S,I)}{\partial I}>0,\qquad \frac{\partial\mathcal{F}(S,I)}{\partial S}>0,\qquad \text{for all}\quad S,I>0.$$

In addition, we find that nonlinear incidence rates (3.21) and (3.22) are concave about the infected fraction I, i.e.

$$\frac{\partial^2 \mathcal{F}_1(S,I)}{\partial I^2} \leq 0, \qquad \frac{\partial^2 \mathcal{F}_2(S,I)}{\partial I^2} \leq 0, \qquad \text{for all} \quad S, I > 0,$$

indicating the saturating effect. Therefore, we infer that cost functionals (3.19) and (3.20) are reasonable, and their corresponding incidence rate includes the saturating effect.

4. Fokker-Planck asymptotic analysis

Following the quasi-invariant limit method in [2], the Fokker-Planck equation can be derived from the Boltzmann-type equation, and the description of the large-time behavior of wealth distribution is obtained through its steady-state solution.

Here, we introduce a scale parameter $0 < \epsilon \ll 1$, and set $\tau = \epsilon t$, $g_H(w,\tau) = f_H(w,t)$, $H \in \{S,I,R\}$. Let $\alpha = \epsilon$, then $\beta = \epsilon/(\gamma + 2\epsilon)$. To preserve the main properties of kinetic Equation (3.1), we employ the scaled quantities

$$\sigma^2 \to \epsilon\sigma^2, \quad \rho(w,v) \to \epsilon\rho(w,v), \quad \kappa \to \epsilon\kappa, \quad r(w) \to \epsilon r(w). \tag{4.1}$$

Then, for any test function $\psi(w) \in C_0^\infty(\mathbb{R}_+)$, the scaled weak form of (3.1) reads

$$\begin{aligned}
\frac{d}{d\tau}\int_{\mathbb{R}_+} g_S(w,\tau)\psi(w)dw = &-\frac{1}{\epsilon}\int_{\mathbb{R}_+} \Xi_\epsilon(w,\tau) g_S(w,\tau)\psi(w)dw \\
&+\frac{1}{\epsilon}\sum_{\Lambda\in\{S,I,R\}}\int_{\mathbb{R}_+} Q_\epsilon(g_S,g_\Lambda)(w,\tau)\psi(w)dw, \qquad (4.2a)\\
\frac{d}{d\tau}\int_{\mathbb{R}_+} g_I(w,\tau)\psi(w)dw = &\frac{1}{\epsilon}\int_{\mathbb{R}_+} \left[\Xi_\epsilon(w,\tau) g_S(w,\tau) - r_\epsilon(w) g_I(w,\tau)\right]\psi(w)dw \\
&+\frac{1}{\epsilon}\sum_{\Lambda\in\{S,I,R\}}\int_{\mathbb{R}_+} Q_\epsilon(g_I,g_\Lambda)(w,\tau)\psi(w)dw, \qquad (4.2b)\\
\frac{d}{d\tau}\int_{\mathbb{R}_+} g_R(w,\tau)\psi(w)dw = &\frac{1}{\epsilon}\int_{\mathbb{R}_+} r_\epsilon(w) g_I(w,\tau)\psi(w)dw \\
&+\frac{1}{\epsilon}\sum_{\Lambda\in\{S,I,R\}}\int_{\mathbb{R}_+} Q_\epsilon(g_R,g_\Lambda)(w,\tau)\psi(w)dw. \qquad (4.2c)
\end{aligned}$$

From (4.1), we have

$$\frac{1}{\epsilon}\int_{\mathbb{R}_+} \Xi_\epsilon(w,\tau) g_S(w,\tau)\psi(w)dw = \int_{\mathbb{R}_+} \Xi(w,\tau) g_S(w,\tau)\psi(w)dw, \tag{4.3}$$

$$\frac{1}{\epsilon}\int_{\mathbb{R}_+} r_\epsilon(w) g_I(w,\tau)\psi(w)dw = \int_{\mathbb{R}_+} r(w) g_I(w,\tau)\psi(w)dw. \tag{4.4}$$

For the collision integral operator Q_ϵ in (4.2), which is given by (3.3), we consider the second-order Taylor expansion of $\psi(w^*)$ around w,

$$\begin{aligned}
&\frac{1}{\epsilon}\int_{\mathbb{R}_+} Q_\epsilon(g_H,g_\Lambda)(w,\tau)\psi(w)dw \\
=&\frac{c_{H\Lambda}}{\epsilon}\int_{\mathbb{R}_+^2}\left\langle \psi'(w)(w^*-w) + \frac{\psi''(w)}{2}(w^*-w)^2\right\rangle g_H(w,\tau) g_\Lambda(v,\tau)dvdw + \mathcal{R}(\epsilon), \qquad (4.5)
\end{aligned}$$

where $H,\Lambda\in\{S,I,R\}$. The residual $\mathcal{R}(\epsilon)$ describes the higher order of ϵ. In fact, for any test function $\psi(\cdot)\in\mathcal{C}_0^{2+\delta}(\mathbb{R}_+)$, we have

$$\begin{aligned}\mathcal{R}(\epsilon)&=\frac{c_{H\Lambda}}{\epsilon}\int_{\mathbb{R}_+^2}\left\langle\frac{\psi''(\tilde{w})-\psi''(w)}{2}(w^*-w)^2\right\rangle g_H(w,\tau)g_\Lambda(v,\tau)dvdw\\&=\mathcal{O}(\epsilon^{1+\delta}),\end{aligned}$$

where $\tilde{w}=\xi w^*+(1-\xi)w$ for some $\xi\in(0,1)$.

From the binary wealth exchange (2.9a), and the scaling $\alpha=\epsilon$, we get

$$\lim_{\epsilon\to0}\frac{1}{\epsilon}\langle w^*-w\rangle=\big[2\theta(1-\gamma_H)-\frac{1}{\gamma}-\gamma_H P(w,H;v,\Lambda)\big]w+\big(\frac{1}{\gamma}+\gamma_\Lambda P(w,H;v,\Lambda)\big)v.$$

Using the scaling $\sigma^2\to\epsilon\sigma^2$, the limitation of (4.5) is expressed as

$$\begin{aligned}&\lim_{\epsilon\to0}\frac{1}{\epsilon}\int_{\mathbb{R}_+}Q_\epsilon(g_H,g_\Lambda)(w,\tau)\psi(w)dw\\=&c_{H\Lambda}\int_{\mathbb{R}_+}\left\{-\frac{\partial}{\partial w}\big[G_{H\Lambda}(w,\tau)g_H(w,\tau)\big]+\frac{\sigma^2}{2}\Lambda(t)\frac{\partial^2}{\partial w^2}\big[w^2g_H(w,\tau)\big]\right\}\psi(w)dw,\end{aligned}\tag{4.6}$$

where

$$\begin{aligned}G_{H\Lambda}(w,\tau)=&\frac{m_\Lambda(\tau)}{\gamma}+\big[2\theta(1-\gamma_H)-\frac{1}{\gamma}\big]\Lambda(t)w\\&+\int_{\mathbb{R}_+}(\gamma_\Lambda\cdot v-\gamma_H\cdot w)P(w,H;v,\Lambda)\cdot g_\Lambda(v,\tau)dv,\end{aligned}$$

and $m_\Lambda(\tau)=\int_{\mathbb{R}_+}wg_\Lambda(v,\tau)dw$ denotes the mean wealth of agents in class Λ.

Substituting (4.3) and (4.4) into (4.2), taking $\epsilon\to0$ and combining with (4.6), from (4.2), we obtain the Fokker-Planck equations

$$\begin{aligned}\frac{\partial g_S(w,\tau)}{\partial\tau}=&-\Xi(w,\tau)g_S(w,\tau)\\&+\sum_{\Lambda\in\{S,I,R\}}c_{S\Lambda}\left\{-\frac{\partial}{\partial w}\big[G_{S\Lambda}(w,\tau)g_S(w,\tau)\big]+\frac{\sigma^2\Lambda(t)}{2}\frac{\partial^2}{\partial w^2}\big[w^2g_S(w,\tau)\big]\right\},\end{aligned}\tag{4.7a}$$

$$\begin{aligned}\frac{\partial g_I(w,\tau)}{\partial\tau}=&\Xi(w,\tau)g_S(w,\tau)-r(w)g_I(w,\tau)\\&+\sum_{\Lambda\in\{S,I,R\}}c_{I\Lambda}\left\{-\frac{\partial}{\partial w}\big[G_{I\Lambda}(w,\tau)g_I(w,\tau)\big]+\frac{\sigma^2\Lambda(t)}{2}\frac{\partial^2}{\partial w^2}\big[w^2g_I(w,\tau)\big]\right\},\end{aligned}\tag{4.7b}$$

$$\begin{aligned}\frac{\partial g_R(w,\tau)}{\partial\tau}=&r(w)g_I(w,\tau)\\&+\sum_{\Lambda\in\{S,I,R\}}c_{R\Lambda}\left\{-\frac{\partial}{\partial w}\big[G_{R\Lambda}(w,\tau)g_R(w,\tau)\big]+\frac{\sigma^2\Lambda(t)}{2}\frac{\partial^2}{\partial w^2}\big[w^2g_R(w,\tau)\big]\right\},\end{aligned}\tag{4.7c}$$

with boundary conditions

$$G_{H\Lambda}(w,\tau)g_H(w,\tau)\big|_{w=0}^{w=\infty}=0$$

and

$$\frac{\partial}{\partial w}\left[w^2 g_H(w,\tau)\right]\Big|_{w=0}^{w=\infty}=0, \qquad H,\Lambda\in\{S,I,R\}.$$

From Proposition 3.1, the steady-state infected fraction is $I^\infty=0$, so the wealth distribution and mean wealth of the infected class are zero, i.e. $g_I^\infty=0$ and $m_I^\infty=0$. We have

$$\Xi^\infty(w)=\int_{\mathbb{R}_+}\rho(w,v)\left[1-\lambda u_{soc}^\infty\right]g_I^\infty(v)dv=0.$$

Therefore, from (4.7a) and (4.7c), the steady-state solution $g_H^\infty(w)$ $\left(H\in\{S,R\}\right)$ satisfies the ordinary differential equation

$$\left(\frac{\sigma^2}{2}\sum_{\Lambda\in\{S,R\}}c_{H\Lambda}\cdot\Lambda^\infty\right)\frac{d}{dw}\left[w^2 g_H^\infty(w)\right]-\left(\sum_{\Lambda\in\{S,R\}}c_{H\Lambda}\cdot G_{H\Lambda}^\infty(w)\right)g_H^\infty(w)=0, \tag{4.8}$$

where

$$\begin{aligned}G_{H\Lambda}^\infty(w)=&\frac{m_\Lambda^\infty}{\gamma}+\left[2\theta(1-\gamma_H)-\frac{1}{\gamma}\right]\Lambda^\infty w\\&+\int_{\mathbb{R}_+}(\gamma_\Lambda\cdot v-\gamma_H\cdot w)P(w,H;v,\Lambda)g_\Lambda^\infty(v)dv.\end{aligned} \tag{4.9}$$

Λ^∞ and m_Λ^∞ represent the steady-state fraction and mean wealth of agents in class $\Lambda\in\{S,R\}$, respectively. Besides, (S^∞,R^∞) is the steady-state solution of the SIR epidemic system (3.7).

Substitute $\psi(w)=w$ into (4.2) and take $\epsilon\to0$, then the steady-state mean wealth m_H^∞ $\left(H\in\{S,R\}\right)$ satisfies

$$\begin{aligned}&\Big(\sum_{\Lambda\in\{S,R\}}c_{H\Lambda}\cdot\Lambda^\infty\Big)\left[2\theta(1-\gamma_H)-\frac{1}{\gamma}\right]m_H^\infty+\frac{H^\infty}{\gamma}\Big(\sum_{\Lambda\in\{S,R\}}c_{H\Lambda}\cdot m_\Lambda^\infty\Big)\\&\quad+\sum_{\Lambda\in\{S,R\}}c_{H\Lambda}\int_{\mathbb{R}_+^2}(\gamma_\Lambda v-\gamma_H w)P(w,H;v,\Lambda)g_H^\infty(w)g_\Lambda^\infty(v)dvdw=0.\end{aligned} \tag{4.10}$$

Remark 4.1. In Remark 3.1, (3.15) describes the time evolution of wealth distribution in an epidemic background with SEIAR compartments. Following the asymptotic limit method above, for the dynamic Equations (3.15), we have $f_E^\infty=f_I^\infty=f_A^\infty=0$. f_S^∞ and f_R^∞ are steady-state solutions of equations

$$\sum_{\Lambda\in\{S,R\}}Q(f_S,f_\Lambda)(w,t)=0, \qquad \sum_{\Lambda\in\{S,R\}}Q(f_R,f_\Lambda)(w,t)=0,$$

which is aligned with the wealth distribution in the SIR compartments model.

Equations (4.9) and (4.10) indicate that the steady-state distribution $g_H^\infty(w)$ $\left(H\in\{S,R\}\right)$ depends on the form of the trading propensity $P(w,H;v,\Lambda)$. Next, we analyze the expression of the steady-state solution of (4.8) through several examples.

4.1. Steady state wealth distribution in a closed economy. According to (2.11), if the trading propensities in (2.9) satisfy $P(w,H;v,\Lambda)=P(v,\Lambda;w,H)$, and saving is not considered, i.e. $\theta=0$, the wealth of the whole agent system is conserved. In this case, the implicit solution of (4.8) is given by

$$g_H^\infty(w)=C_H\cdot w^{-2-\frac{2}{\gamma\sigma^2}}\cdot\exp\left\{\int\frac{2\sum\limits_{\Lambda\in\{S,R\}}c_{H\Lambda}\tilde{G}_{H\Lambda}^\infty(w)}{(\sigma^2\sum\limits_{\Lambda\in\{S,R\}}c_{H\Lambda}\cdot\Lambda^\infty)w^2}dw\right\},\qquad H\in\{S,R\},\quad(4.11)$$

where

$$\tilde{G}_{H\Lambda}^\infty(w)=\frac{m_\Lambda^\infty}{\gamma}+\int_{\mathbb{R}_+}P(w,H;v,\Lambda)(\gamma_\Lambda v-\gamma_H w)g_\Lambda^\infty(v)dv$$

and the positive constant C_H satisfies $\int_{\mathbb{R}_+}g_H^\infty(w)dw=H^\infty$. The mean wealth of the whole agent system $m=m_S^\infty+m_R^\infty$ is time invariant.

To study the impact of exchange behavior on wealth inequality, in which trading propensity is affected by the wealth of both traders, we consider two simple cases, namely, the trading propensity $P(w,H;v,\Lambda)$ is a monotonic increasing or decreasing function of wealth. Let the contact rate $\rho(w,v)=\rho$ and the recover rate $r(w)=r$ be constants, and $c_{H\Lambda}=1$ $\big(H,\Lambda\in\{S,I,R\}\big)$.

Example 4.1. If trading propensity $P(w,H;v,\Lambda)$ is a decreasing function of wealth w and v, we choose

$$P(w,H;v,\Lambda)=P_{H\Lambda}\cdot\frac{1}{(1+w)(1+v)},$$

where the constant $P_{H\Lambda}\in(0,1]$. Then the agents' steady-state wealth distribution in class $H\in\{S,R\}$ is

$$g_H^\infty(w)=C_H\cdot w^{-2-\frac{2}{\gamma\sigma^2}}\cdot\left(\frac{w}{1+w}\right)^{-\hat{d}_H}e^{-\frac{\hat{b}_H}{w}},\qquad(4.12)$$

where

$$\hat{b}_H=\frac{2m}{\gamma\sigma^2}+\frac{2}{\sigma^2}\cdot\sum_{\Lambda\in\{S,R\}}\big(P_{H\Lambda}\cdot\gamma_\Lambda B_{1,\Lambda}^\infty\big),\qquad\hat{d}_H=\frac{2}{\sigma^2}\cdot\sum_{\Lambda\in\{S,R\}}P_{H\Lambda}\cdot\big(\gamma_\Lambda B_{1,\Lambda}^\infty+\gamma_H B_{0,\Lambda}^\infty\big)$$

and

$$B_{0,\Lambda}^\infty=\int_{\mathbb{R}_+}\frac{1}{1+v}g_\Lambda^\infty(v)dv,\qquad B_{1,\Lambda}^\infty=\int_{\mathbb{R}_+}\frac{v}{1+v}g_\Lambda^\infty(v)dv=\Lambda^\infty-B_{0,\Lambda}^\infty.$$

Example 4.2. If trading propensity $P(w,H;v,\Lambda)$ is an increasing function of wealth w and v, we choose

$$P(w,H;v,\Lambda)=P_{H\Lambda}\cdot\big(1-\frac{1}{1+w}\big)\cdot\big(1-\frac{1}{1+v}\big).$$

Then the steady-state wealth distribution of agents in class $H\in\{S,R\}$ is

$$g_H^\infty(w)=C_H\cdot w^{-2-\frac{2}{\gamma\sigma^2}}(1+w)^{-\check{b}_H}\cdot\left(\frac{w}{1+w}\right)^{\check{d}_H}e^{-\frac{2m}{\gamma\sigma^2}\cdot\frac{1}{w}},\qquad(4.13)$$

where

$$\check{b}_H = \frac{2\gamma_H}{\sigma^2} \sum_{\Lambda\in\{S,R\}} \left(P_{H\Lambda}\cdot B^\infty_{1,\Lambda}\right) \qquad \text{and} \qquad \check{d}_H = \frac{2}{\sigma^2} \sum_{\Lambda\in\{S,R\}} P_{H\Lambda}\cdot\gamma_\Lambda(m^\infty_\Lambda - B^\infty_{1,\Lambda}).$$

The Pareto index of wealth distribution $g^\infty_H(w)$ obtained in Examples 4.1 and 4.2 are $1+2/(\gamma\sigma^2)$ and $1+2/(\gamma\sigma^2)+\check{b}_H$, respectively. Obviously, these two Pareto indexes decrease with the control parameter γ, because a smaller Pareto index means greater wealth inequality. Formulas (4.12) and (4.13) indicate that the feedback control in the form of (2.7), in which the government redistributes all tax revenue, reduces wealth inequality. In addition, the wealth inequality is improved with the increase of the government's control over economic behavior (i.e. γ decreases from ∞ to 0). On the other hand, we find that the Pareto index of (4.12) is less than that of (4.13). As a result, if the rich save more, the wealth inequality may not be improved.

From Proposition 3.3, the contact control u_{soc} affects steady-state fractions S^∞ and R^∞. According to (4.10), the impact of contact control u_{soc} on average wealth m^∞_H $\left(H\in\{S,R\}\right)$ is indirectly reflected by fractions S^∞ and R^∞. Furthermore, the explicit expressions of average wealth m^∞_H and steady-state distribution g^∞_H are closely related to the form of trading propensity $P(\cdot,\cdot;\cdot,\cdot)$. Even in Examples 4.1 and 4.2, where their symmetric trading propensity $P(w,H;v,\Lambda)$ provides us a rough judgment on the shape of the stationary distribution, no explicit expression for g^∞_H is obtained. As a special case, when trading propensity $P(\cdot,\cdot;\cdot,\cdot)$ is a constant, (4.11) provides an explicit form of the distribution g^∞_H.

EXAMPLE 4.3. If the trading propensities $P(w,H;v,\Lambda)=P_{H\Lambda}$ $\left(H,\Lambda\in\{S,I,R\}\right)$ are constants, then the steady-state wealth distribution of agents in class $H\in\{S,R\}$ is explicitly expressed as

$$g^\infty_H(w) = H^\infty \frac{b_H^{a_H}}{\Gamma(a_H)} w^{-a_H-1} e^{-\frac{b_H}{w}}, \tag{4.14}$$

where

$$a_H = 1+\frac{2}{\gamma\sigma^2}+2\gamma_H\left(\sum_{\Lambda\in\{S,R\}} c_{H\Lambda}P_{H\Lambda}\cdot\Lambda^\infty\right)\Big/\left(\sigma^2\sum_{\Lambda\in\{S,R\}} c_{H\Lambda}\cdot\Lambda^\infty\right),$$
$$b_H = 2\left[\sum_{\Lambda\in\{S,R\}} (\frac{1}{\gamma}+\gamma_\Lambda P_{H\Lambda})c_{H\Lambda}\cdot m^\infty_\Lambda\right]\Big/\left(\sigma^2\sum_{\Lambda\in\{S,R\}} c_{H\Lambda}\cdot\Lambda^\infty\right),$$

and the mean wealth m^∞_S and m^∞_R are given by

$$m^\infty_S = \frac{(\frac{1}{\gamma}+\gamma_R P_{SR})S^\infty m}{\frac{1}{\gamma}+(\gamma_R S^\infty+\gamma_S R^\infty)P_{SR}}, \qquad m^\infty_R = \frac{(\frac{1}{\gamma}+\gamma_S P_{SR})R^\infty m}{\frac{1}{\gamma}+(\gamma_R S^\infty+\gamma_S R^\infty)P_{SR}}.$$

Thus, the steady-state wealth distribution of a closed economy reads

$$g^\infty(w) = S^\infty \frac{b_S^{a_S}}{\Gamma(a_S)} w^{-a_S-1} e^{-\frac{b_S}{w}} + R^\infty \frac{b_R^{a_R}}{\Gamma(a_R)} w^{-a_R-1} e^{-\frac{b_R}{w}}. \tag{4.15}$$

From an economic perspective, the shape parameter a_H of the inverse gamma distribution (4.14) characterizes the Pareto index of the wealth distribution for agents with infection state H. Let $c_{H\Lambda}=1$ $\left(H,\Lambda\in\{S,I,R\}\right)$, we get

$$a_S = 1+\frac{2}{\gamma\sigma^2}+\frac{2\gamma_S}{\sigma^2}[P_{SR}+(P_{SS}-P_{SR})S^\infty],$$

$$a_R = 1 + \frac{2}{\gamma\sigma^2} + \frac{2\gamma_R}{\sigma^2}[P_{RR} + (P_{SR} - P_{RR})S^\infty].$$

Considering that the recovered agents have immunity and the susceptible are exposed to have the risk of being infected, we assume that the trading propensity is the largest when both traders are recovered, and the trading propensity is the smallest when both traders are susceptible, i.e. $P_{RR} \geq P_{SR} \geq P_{SS}$. Then, Pareto index a_H, $\big(H \in \{S,R\}\big)$ decreases with the susceptible fraction S^∞. Additionally, Proposition 3.3 indicates that the government's contact control measures u_{soc} makes the steady-state susceptible fraction S^∞ greater than that without control. Therefore, the contact control measures taken by the government to curb the epidemic may aggravate wealth inequality.

Combining with the improving effect of the government's economic control measures on wealth inequality, which is verified in Examples 4.1 and 4.2, we think that while the government takes contact control measures, it is necessary to implement wealth inequality control measures (taxation and redistribution) to avoid economic recession.

4.2. Quasi-stationary state wealth distribution in an open economy. The wealth exchange dynamics discussed in Section 4.1 are in a closed economy, in which the wealth is conserved, and the resulting stationary solution (4.11) describes the Pareto tail property of wealth distribution. However, in an open economy, the wealth is not conserved, the stationary solution of the wealth exchange model (3.1) cannot be obtained. We use the following example, which allows the model (3.1) to have a self-similar solution, to study the large-time behavior of wealth exchange dynamics in an open economy.

EXAMPLE 4.4. Assuming that trading propensity is a symmetric function, i.e. $P(w,H;v,\Lambda) = P(v,\Lambda;w,H)$, agents in different infectious group share a common saving propensity $\gamma_S = \gamma_I = \gamma_R = \gamma_0 < 1$, and savings interest rate $\theta > 0$.

Let $c_{H\Lambda} = 1$ with $H,\Lambda \in \{S,I,R\}$, and denote the mean wealth of the whole agent system as $m(t) := \sum_{H\in\{S,I,R\}} m_H(t)$. Substituting $\psi(w) = w$ into (3.2), and summing the Equations (3.2a - 3.2c) yield

$$\frac{dm(t)}{dt} = 2\alpha\theta(1-\gamma_0)m(t),$$

implying that mean wealth $m(t)$ is not conserved, but increases exponentially with the rate $2\alpha\theta(1-\gamma_0)$. According to the construction method of self-similar solution in [35], we set $\tilde{f}_H(w,t) = m(t) f_H(m(t)w,t)$ $\big(H \in \{S,I,R\}\big)$, which provides

$$\int_{\mathbb{R}_+} \tilde{f}_H(w,t)dw = H(t) \qquad \text{and} \qquad \sum_{H\in\{S,I,R\}} \int_{\mathbb{R}_+} w\tilde{f}_H(w,t)dw = 1.$$

Using the scaled quantities in (4.1), we can repeat the Fokker-Planck asymptotic analysis for $\tilde{f}_H(w,t)$ and obtain the Fokker-Planck system of the evolution process of $\tilde{g}_H(w,\tau) = \tilde{f}_H(w,t)$. Since the infected fraction $I^\infty = 0$, we have $\tilde{g}_I^\infty(w) = 0$. Let trading propensity $P(w,H;v,\Lambda) = P_{H\Lambda}$ be a constant, the steady-state distribution $\tilde{g}_H^\infty(w)$ $\big(H \in \{S,R\}\big)$ satisfies the equation

$$\Big[\big(\tfrac{1}{\gamma} + \gamma_0 \sum_{\Lambda\in\{S,R\}} P_{H\Lambda}\cdot\Lambda^\infty + \sigma^2\big)w - \big(\gamma_0 \sum_{\Lambda\in\{S,R\}} P_{H\Lambda}\cdot\tilde{m}_\Lambda^\infty + \tfrac{1}{\gamma}\big)\Big]\tilde{g}_H^\infty(w) + \tfrac{\sigma^2}{2}w^2\tfrac{d}{dw}\tilde{g}_H^\infty(w) = 0.$$

We get

$$\tilde{g}_H^{\infty}(w) = H^{\infty} \frac{\tilde{b}_H^{\tilde{a}_H}}{\Gamma(\tilde{a}_H)} w^{-\tilde{a}_H - 1} e^{-\frac{\tilde{b}_H}{w}}, \tag{4.16}$$

where

$$\tilde{a}_H = \frac{2}{\sigma^2}\Big(\frac{1}{\gamma} + \gamma_0 \sum_{\Lambda \in \{S,R\}} P_{H\Lambda} \cdot \Lambda^{\infty}\Big) + 1, \qquad \tilde{b}_H = \frac{2}{\sigma^2}\Big(\frac{1}{\gamma} + \gamma_0 \sum_{\Lambda \in \{S,R\}} P_{H\Lambda} \cdot \tilde{m}_{\Lambda}^{\infty}\Big),$$

and $\tilde{m}_{\Lambda}^{\infty} = \int_{\mathbb{R}_+} w \tilde{g}_{\Lambda}^{\infty}(w) dw$.

The wealth exchange dynamics (3.1) in an open economy has a non-trivial quasi-stationary state wealth distribution

$$\tilde{g}^{\infty}(w) = S^{\infty} \frac{\tilde{b}_S^{\tilde{a}_S}}{\Gamma(\tilde{a}_S)} w^{-\tilde{a}_S - 1} e^{-\frac{\tilde{b}_S}{w}} + R^{\infty} \frac{\tilde{b}_R^{\tilde{a}_R}}{\Gamma(\tilde{a}_R)} w^{-\tilde{a}_R - 1} e^{-\frac{\tilde{b}_R}{w}} \tag{4.17}$$

and the large-time behavior of the distribution shows a Pareto tail.

In the form of the Pareto index $\tilde{a}_H$ of the wealth distribution for agents in class H, it is noted that the impact of the government's epidemic and economic control measures on wealth inequality is consistent with the results of wealth exchange dynamics in the closed economy in Example 4.3. In particular, if $\gamma_S = \gamma_I = \gamma_R = \gamma_0$ in (4.14), distributions (4.16) and (4.14) have the same Pareto index, i.e. $a_H = \tilde{a}_H$.

5. Numerical experiments

In the following simulations, if there is no special declaration, we always take the initial infected fraction $I_0 = 0.01$ and the susceptible fraction $S_0 = 0.99$. In addition, it is assumed that the government's contact control strategies are fully implemented, i.e. $\lambda = 1$.

5.1. Test 1: The impact of contact control on epidemic dynamics. The spread of the epidemic has a negative impact on people's lives. Before the popularization of vaccines, the government usually took non-drug measures to curb the spread of the virus. Using the feedback control method, we introduce the feedback control SIR model (3.7) with a general form of contact control (3.9). To verify the results in Section 3.1, which show the positive impact of government's contact control measures on curbing the epidemic, we compare the SIR model (3.7) with the classical SIR model (3.12) in Figure 5.1.

From (3.21) and (3.22), the saturated incidence rates $\mathcal{F}_1(S,I)$ and $\mathcal{F}_2(S,I)$ are monotonically increasing functions of p_1 and p_2, respectively. Since $\mathcal{F}_2(S,I)$ decreases monotonically with respect to the parameter q, we take $q = 1/2$ in the following simulations. In the first row of Figure 5.1, we take the epidemiological parameters $\rho = 0.25$ and $r = 0.1$, namely, the average recovery time is set to 10 days as in [5, 6]. In the second row of Figure 5.1, we take $\rho = 0.3$ and $r = 0.05$, which are close to the COVID-19 epidemiological parameters of some European countries, such as Italy, France and Spain (see [5,16]). In the first column of Figure 5.1, we simulate the dynamics of the susceptible fraction $S(t)$ and the infected fraction $I(t)$ of the feedback control SIR model (3.7) when parameters $p_1 = 0.5, 1$ and $p_2 = 1, 2$, and the comparison of corresponding incidence rates is shown in the second column. The images inserted in Figure 5.1(b) and (d) verify the non-negativity of $\partial\mathcal{F}_2/\partial S$ and $\partial\mathcal{F}_2/\partial I$. Figure 5.1(a) and (c) illustrate that the steady-state susceptible fraction and epidemic duration corresponding to incidence rate $\mathcal{F}_1(S,I)$ ($\mathcal{F}_2(S,I)$) decrease with respect to parameter p_1 (p_2), while the peak of the

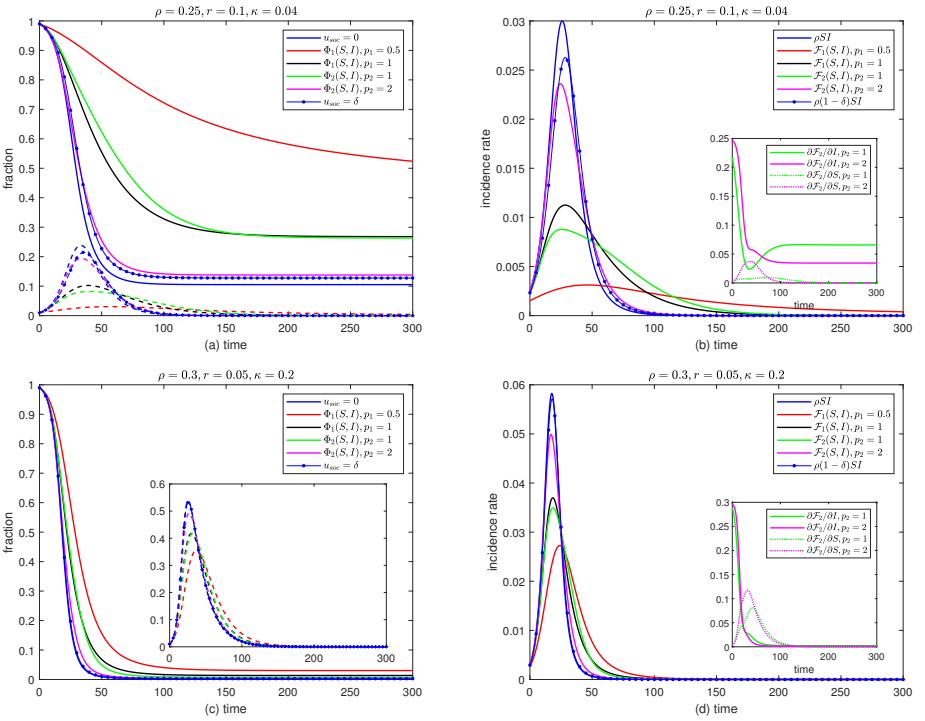

FIG. 5.1. (a) and (c): *The solid line and double dashed line respectively represent the dynamics of the susceptible and infected fraction under different contact control measures.* (b) and (d): *The incidence rate of epidemic models in (a) and (c), respectively.*

infected fraction increases with p_1 (p_2). Therefore, in terms of the epidemic duration and the peak of the infected fraction, contact control measures corresponding to $p_1 = 1$ or $p_2 = 1$ perform better.

Note that incidence rates (3.21) and (3.22) are time-varying functions related to the infected fraction. For comparison, we consider the SIR model (3.7) with a fixed contact control $u_{soc} = \delta \in [0,1)$, which measures the intensity of the fixed control adopted by the government and is taken as the maximum of the initial control value corresponding to the incidence rates (3.21) and (3.22) when $p_1 = p_2 = 1$, i.e.

$$\delta = \max\left\{1 - \frac{1}{1+cI_0}, cS_0^{1-q}I_0\right\}. \tag{5.1}$$

The corresponding epidemic dynamics are shown in Figure 5.1.

Figure 5.1 provides results, which are consistent with the Propositions 3.1, 3.3 and 3.4, indicating that the feedback control SIR model (3.7) has a steady-state solution, and the contact control measures taken by the government can reduce the peak of the infected fraction and keep more agents in an uninfected state. However, the dynamics of infected fractions in Figure 5.1(a,c) and the incidence rates in Figure 5.1(b,d) suggest that the implementation of contact control measures leads to a delay of the epidemic's end time. From Figure 5.1, we find that compared with the fixed contact control (5.1), time-varying contact controls involved in (3.21) and (3.22) have a better effect on preventing virus transmission.

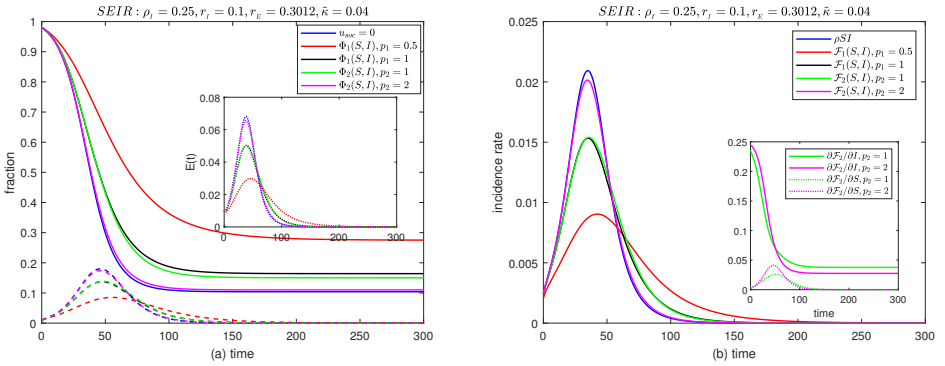

FIG. 5.2. (a): *The solid line and double dashed line respectively represent the dynamics of the susceptible and infected fraction under different contact control measures, the inserted image represents the dynamics of exposed fraction.* (b): *The incidence rate of epidemic models in (a).*

In a SEIR epidemic model (3.17) with contact control (3.6) and cost functionals (3.19) and (3.20), the time evolution of susceptible, exposed and infected fractions and the corresponding incidence rate are depicted in Figure 5.2. Take $I_0 = E_0 = 0.01$, $S_0 = 0.98$ and $r_E = 0.3012$, which means the incubation period is 3.32 days [5,17]. Figure 5.2 shows that the steady-state exposed fraction E^∞ and infected fraction I^∞ are zero, and the impact of contact control on SIER epidemic dynamics is the same as that of SIR model.

In (4.15), the steady-state wealth distribution is affected by the stationary susceptible fraction S^∞. To qualitatively analyze the impact of epidemic control on wealth distribution more clearly, and to obtain the possible bimodal wealth distribution that may occur when multiple groups of agents exist (see [14,15]), we use $\rho = 0.25$ and $r = 0.1$ in the following simulations.

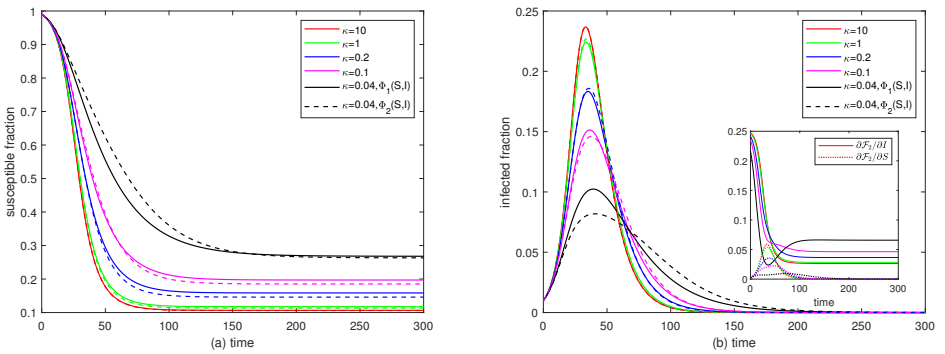

FIG. 5.3. *Influence of contact control parameter κ on epidemic dynamics under contact control measures Φ_1 and Φ_2.*

The expressions of incidence rates (3.21) and (3.22) state that the parameter κ takes a key role in the government's decision of contact control measures. In Figure 5.3, we simulate the epidemic model (3.7) when the incidence rate is $\mathcal{F}_1(S,I)$ and $\mathcal{F}_2(S,I)$, respectively, where $p_1 = p_2 = 1$ and $\kappa \in \{10, 1, 0.2, 0.1, 0.04\}$. The image inserted in Figure 5.3(b) verifies the non-negativity of $\partial\mathcal{F}_2/\partial S$ and $\partial\mathcal{F}_2/\partial I$. Figure 5.3 states that with

the increase of the government's contact control, i.e. the control parameter κ decreases from 10 to 0.04, the steady-state susceptible fraction S^∞ gradually increases, and the peak of the infected fraction decreases. However, the duration of the epidemic extends with the increase of the contact control. In addition, as can be seen from Figure 5.3, when the control degree is large, such as $\kappa = 0.04$, the control measures corresponding to the incidence rate $\mathcal{F}_2(S,I)$ have a more obvious containment effect on the epidemic. For example, when $\kappa = 0.04$, the epidemic duration and the stationary susceptible fraction under both control strategies are similar. However, in the case of the incidence rate $\mathcal{F}_2(S,I)$, the peak of infected fraction is lower and the number of susceptible persons declines more slowly during the epidemic.

5.2. Test 2: The impact of feedback controls on wealth distribution. In Figure 5.4, using the Monte Carlo method, we verify that the equilibrium solution (4.15) of the Fokker-Planck Equations (4.7) asymptotically approximates the solution of the Boltzmann Equation (3.1) at final time T when the scale parameter ϵ is sufficiently small. In the simulation, the number of the whole agent system is 10^5. We take $p_1 = 1$, $\gamma_R = 0.3$, $\gamma_S = 0.075$, $P_{RR} = 1$, $P_{SR} = 0.7$, $P_{SS} = 0.5$ and $\gamma = \infty$. These values of saving propensities and exchange propensities are due to the fact that susceptible agents have a higher risk of infection than the recovered individuals who have been immunized, so they are more careful in the transaction.

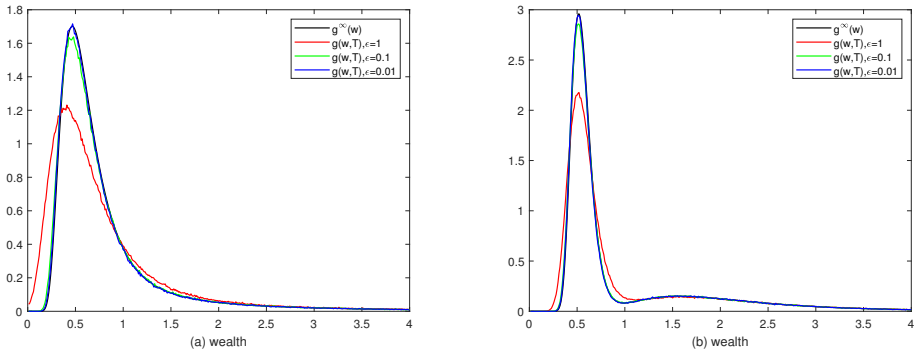

FIG. 5.4. *Comparison between the equilibrium solution (4.15) of the Fokker-Planck Equations (4.7) and the solution of the Boltzmann Equation (3.1) at time T with scale parameters $\epsilon = 1, 0.1, 0.01$.* (a): $\sigma^2 = 0.1$ *and* $\kappa = 0.1$. (b): $\sigma^2 = 0.02$ *and* $\kappa = 0.04$.

In Section 4.1, the steady-state (self-similar) solutions (4.15) and (4.17) of the wealth exchange dynamics (3.7) show that the Pareto index decreases with the strengthening of the government's contact control measures, suggesting the aggravation of wealth inequality. Gini coefficient and Palma ratio are important parameters to measure the wealth inequality. The Gini coefficient belongs to $[0,1]$, and a larger Gini coefficient indicates a more unequal distribution of wealth. The Parma ratio is the ratio of the wealth of the richest 10% of the population to the wealth of the poorest 40%. Define the Lorenz curve as [15]

$$L(F(w)) = \int_0^w v g^\infty(v) dv, \qquad F(w) = \int_0^w g^\infty(v) dv,$$

then the Gini coefficient is

$$Gini = 1 - 2\int_0^1 L(F(w))dF(w)$$

and the Parma ratio is equal to $[1 - L(F(w) = 0.9)]/L(F(w) = 0.4)$.

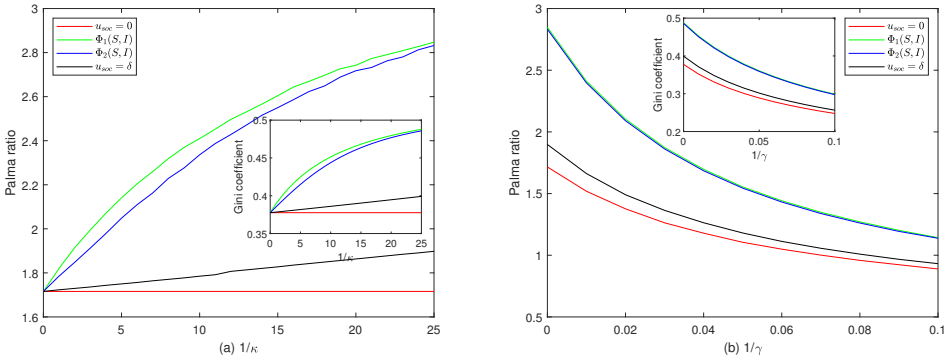

FIG. 5.5. *The variation of wealth inequality index of distribution (4.15), such as Gini coefficient and Parma ratio, with parameters κ and γ.* (a): $\gamma = \infty$. (b): $\kappa = 0.04$.

Under different contact controlling measures in Figure 5.1(a), Figure 5.5 shows the influence of contact control parameter κ and economic control parameter γ on wealth inequality, where $p_1 = p_2 = 1$, $q = 1/2$, $\sigma^2 = 0.1$, and the other parameters are the same as in Figure 5.4. $\kappa = \infty$ and $\gamma = \infty$ correspond to the situations without contact control and economic regulation, respectively. The larger $1/\kappa$ or $1/\gamma$, the stronger the control intensity. In Figure 5.5(a), compared with the situation without contact control, the Palma ratio under the three contact controls almost increases with respect to $1/\kappa$, and the Gini coefficient increases monotonically with respect to $1/\kappa$. This suggests that increased contact control may exacerbate wealth inequality. In Figure 5.5(b), the Palma ratio and Gini coefficient under different contact control measures are monotonically decreasing about $1/\gamma$, indicating that the increase of economic regulation intensity may improve the inequality of wealth distribution. In addition, for any fixed parameter κ or γ, the Parma ratio and Gini coefficient corresponding to Φ_2 are almost less than that of Φ_1. Therefore, from the comprehensive consideration of economic perspective and epidemic containment level, we think that the contact control measure corresponding to Φ_2 (i.e., the incidence rate $\mathcal{F}_2(S,I)$) with $p_2 = 1$ is better than that corresponding to Φ_1.

Figure 5.6 depicts the effects of parameters γ and κ on the wealth distribution (4.15), where we take Φ_2 with $p_2 = 1$, and the other parameter values are the same as Figure 5.4. In Figure 5.6, for each fixed risk parameter σ^2, with the enhancement of contact control (i.e., the decrease of κ), the wealth distribution curve shifts to the left and the Lorentz curve deviates from the equality line. The number of poor people increases and the wealth of the middle and lower classes decreases, indicating the worsening of wealth inequality. As the intensity of economic regulation increases (i.e., γ decreases), the wealth distribution curve shifts to the right, the Lorentz curve approaches the equality line. The number of agents at both low and high wealth levels has decreased, and the wealth of the middle and lower classes increased, indicating

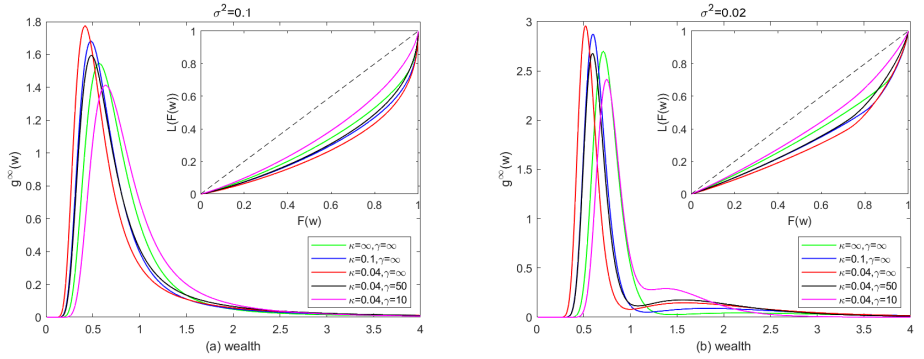

FIG. 5.6. *Steady-state wealth distribution (4.15) and Lorentz curve for different values of parameters κ and γ.*

an improvement in wealth inequality. Therefore, to avoid the negative impact of contact control measures on wealth distribution, appropriate economic measures, such as taxation and redistribution, should be considered simultaneously by the government. In addition, under appropriate parameters, the wealth distribution of the whole agent system presents a bimodal distribution. When $\sigma^2 = 0.02$, Figure 5.6(b) shows that the increase of contact control intensity promotes the emergence of a bimodal distribution curve, and the bimodal distribution gradually becomes a unimodal distribution with the strengthening of economic regulation.

6. Conclusions

Inspired by the study of wealth distribution under infectious spread in [15], we introduce and discuss a multi-agent wealth exchange model with controls for infectious diseases and wealth inequality. Before the popularization of vaccines, non-pharmaceutical interventions, which reduce contact between individuals, played a significant role in controlling the epidemic. Our analysis illustrates that comparing with the situation without control, the implementation of contact control measures reduces the peak of infected fraction, and makes more agents remain uninfected. Unfortunately, the implementation of contact control and the increase of control intensity may prolong the epidemic's duration, and may aggravate wealth inequality. In particular, the wealth status of most agents at middle and low levels becomes worse.

With two introduced cost functions, which are the increasing concave function and the increasing convex function of the infected fraction, respectively, we obtain two nonlinear incidence rates $\mathcal{F}_1(S,I)$ and $\mathcal{F}_2(S,I)$ of the feedback control SIR model, and verify that these two incidence rates satisfy the biologically feasible conditions and include the saturating effect. Considering the economic benefits and the containment effect of the epidemic (such as the duration of epidemic and the peak of the infected fraction), numerical experiments show that the contact control strategy corresponding to the incidence rate $\mathcal{F}_2(S,I)$, $p_2 = 1$ performs well.

In the multi-agent wealth exchange model, the trading propensity relies on the infection status and the wealth of the two trading agents. The government's economic measure (such as taxation and redistribution), which is implemented to narrow the wealth gap, is also considered. Via the quasi invariant limit method, the Boltzmann-type system describing the wealth dynamics is transformed into Fokker-Planck equations, whose steady-state (self-similar) solution for a closed (an open) economy presents the

Pareto tail of wealth distribution. Examples of a closed economy, in which an agent's trading propensity depends on the wealth of both traders, suggest that if the rich allocate more wealth in savings, the degree of wealth inequality may increase. Numerical experiments show that economic control measures can alleviate wealth inequality caused by contact control. With the enhancement of government economic control, the wealth status of agents at low and middle levels is improved obviously.

It is worth noting that our work verifies the views of Dosi et al. [18] from the perspective of mathematical models. For example, the prevalence of COVID-19 may aggravate wealth inequality, and redistribution policies are needed to avoid the outbreak of social inequality.

Acknowledgments. This research is supported by the National Natural Science Foundation of China (No. 11471263) and Sichuan Science and Technology Program (Grant No. 2023NSFSC1343). The authors are very grateful to the reviewers for their valuable and meaningful comments for the paper.

REFERENCES

[1] G. Albi, M. Herty, and L. Pareschi, *Kinetic description of optimal control problems and applications to opinion consensus*, Commun. Math. Sci., 13(6):1407–1429, 2015. 1, 2.1

[2] G. Albi, L. Pareschi, G. Toscani, and M. Zanella, *Recent advances in opinion modeling: Control and social influence*, in N. Bellome, P. Degond, and E. Tadmor (eds.), Active Particles, Volume 1. Modeling and Simulation in Science, Engineering and Technology. Birkhäuser, Cham., 49–98, 2017. 1, 4

[3] G. Albi, L. Pareschi, and M. Zanella, *Boltzmann type control of opinion consensus through leaders*, Phil. Trans. R. Soc. A, 372(2028):20140138, 2014. 1, 2.1

[4] G. Albi, L. Pareschi, and M. Zanella, *Boltzmann games in heterogeneous consensus dynamics*, J. Stat. Phys., 175:97–125, 2019. 1

[5] G. Albi, L. Pareschi, and M. Zanella, *Modelling lockdown measures in epidemic outbreaks using selective socio-economic containment with uncertainty*, Math. Biosci. Eng., 18(6):7161–7190, 2021. 1, 3.1, 3.2, 5.1, 5.1

[6] G. Albi, L. Pareschi, and M. Zanellaz, *Control with uncertain data of socially structured compartmental epidemic models*, J. Math. Biol., 82(7):1–41, 2021. 1, 3.1, 5.1

[7] M.L. Bertotti, *Modelling taxation and redistribution: A discrete active particle kinetic approach*, Appl. Math. Comput., 217(2):752–762, 2010. 1

[8] W. Boscheri, G. Dimarco, and L. Pareschi, *Modeling and simulating the spatial spread of an epidemic through multiscale kinetic transport equations*, Math. Model. Meth. Appl. Sci., 31(6):1059–1097, 2021. 1

[9] C. Brugna and G. Toscani, *Kinetic models for goods exchange in a multi-agent market*, Phys. A, 499(2):362–375, 2018. 1

[10] S. Cordier, L. Pareschi, and G. Toscani, *On a kinetic model for a simple market economy*, J. Stat. Phys., 120(1-2):253–277, 2005. 1, 1

[11] B. Düring, P. Markowich, J.-F. Pietschmann, and M.-T. Wolfram, *Boltzmann and Fokker-Planck equations modelling opinion formation in the presence of strong leaders*, Proc. R. Soc. A-Math. Phys., 465(2112):3687–3708, 2009. 2.1

[12] B. Düring, L. Pareschi, and G. Toscani, *Kinetic models for optimal control of wealth inequalities*, Eur. Phys. J. B, 91(10):265, 2018. 1, 1, 2.1, 2.1

[13] B. Düring and G. Toscani, *Hydrodynamics from kinetic models of conservative economies*, Phys. A, 384(2):493–506, 2007. 1

[14] B. Düring and G. Toscani, *International and domestic trading and wealth distribution*, Commun. Math. Sci., 6(4):1043–1058, 2008. 1, 2.1, 3, 5.1

[15] G. Dimarco, L. Pareschi, G. Toscani, and M. Zanella, *Wealth distribution under the spread of infectious diseases*, Phys. Rev. E, 102:022303, 2020. 1, 1, 2.1, 3, 3.1, 5.1, 5.2, 6

[16] G. Dimarco, B. Perthame, G. Toscani, and M. Zanella, *Kinetic models for epidemic dynamics with social heterogeneity*, J. Math. Biol., 83(1):1–32, 2021. 1, 5.1

[17] G. Dimarco, G. Toscani, and M. Zanella, *Optimal control of epidemic spreading in the presence of social heterogeneity*, Phil. Trans. R. Soc. A, 380:20210160, 2022. 1, 3.1, 5.1

[18] G. Dosi, L. Fanti, and M.E. Virgillito, *Unequal societies in usual times, unjust societies in pandemic ones*, J. Ind. Bus. Econ., 47:371–389, 2020. 1, 6

[19] P. van den Driessche and J. Watmough, *A simple SIS epidemic model with a backward bifurcation*, J. Math. Biol., 40(6):525–540, 2000. 3.2

[20] M.S. Eichenbaum, S. Rebelo, and M. Trabandt, *The macroeconomics of epidemics*, Rev. Financ. Stud., 34(11):5149–5187, 2021. 1

[21] N.M. Ferguson, D.A.T. Cummings, C. Fraser, J.C. Cajka, P.C. Cooley, and D.S. Burke, *Strategies for mitigating an influenza pandemic*, Nature, 422:448–452, 2006. 1

[22] G. Furioli, A. Pulvirenti, E. Terraneo, and G. Toscani, *Fokker-Planck equations in the modeling of socio-economic phenomena*, Math. Model. Meth. Appl. Sci., 27(01):115–158, 2016. 1, 1

[23] G. Furioli, A. Pulvirenti, E. Terraneo, and G. Toscani, *Non-Maxwellian kinetic equations modeling the dynamics of wealth distribution*, Math. Model. Meth. Appl. Sci., 30(4):685–725, 2020. 1

[24] S. Gualandi and G. Toscani, *Human behavior and lognormal distribution. A kinetic description*, Math. Model. Meth. Appl. Sci., 29(4):717–753, 2019. 1

[25] H.W. Hethcote, *Qualitative analyses of communicable disease models*, Math. Biosci., 28(3-4):335–356, 1976. 1, 3

[26] H.W. Hethcote, *The mathematics of infectious diseases*, SIAM Rev., 42(4):599–653, 2000. 1, 3

[27] H.W. Hethcote and S.A. Levin, *Three basic epidemiological models*, in S.A. Levin, T.G. Hallam, and L.J. Gross (eds.), Applied Mathematical Ecology, Springer Berlin Heidelberg, 18:119–144, 1989. 1, 3, 3.1, 3.1

[28] T.D. Hollingsworth, D. Klinkenberg, H. Heesterbeek, and R.M. Anderson, *Mitigation strategies for pandemic influenza A: Balancing conflicting policy objectives*, PloS Comput. Biol., 7(2):e1001076, 2011. 1

[29] W.O. Kermack and A.G. Mckendrick, *A contribution to the mathematical theory of epidemics*, Proc. R. Soc. A Math. Phys., 115(772):700–721, 1927. 1

[30] A. Korobeinikov and P.K. Maini, *Non-linear incidence and stability of infectious disease models*, Math. Med. Biol., 22(2):113–128, 2005. 1, 3.2, 3.2

[31] S. Lee, G. Chowell, and C. Castillo-Chávez, *Optimal control for pandemic influenza: The role of limited antiviral treatment and isolation*, J. Theor. Biol., 265:136–150, 2010. 1

[32] X. Liu and P. Stechlinski, *Infections disease models with time-varying parameters and general nonlinear incidence rate*, Appl. Math. Model., 36:1974–1994, 2012. 1, 3.2

[33] D. Matthes and G. Toscani, *On steady distributions of kinetic models of conservative economies*, J. Stat. Phys., 130(6):1087–1117, 2008. 1

[34] D.Q. Mayne and H. Michalska, *Receding horizon control of nonlinear systems*, IEEE Trans. Automat. Control, 35(7):814–824, 1990. 2.1

[35] L. Pareschi and G. Toscani, *Self-similarity and power-like tails in nonconservative kinetic models*, J. Stat. Phys., 124(2-4):747–779, 2006. 4.4

[36] L. Pareschi and G. Toscani, *Wealth distribution and collective knowledge: A Boltzmann approach*, Phil. Trans. R. Soc. A, 372(2028):20130396, 2014. 1, 2.1

[37] T.A. Perkins and G. España, *Optimal control of the COVID-19 pandemic with non-pharmaceutical interventions*, Bull. Math. Biol., 82(9):118, 2020. 1

[38] S.L. Polk and B.M. Boghosian, *The nonuniversality of wealth distribution tails near wealth condensation criticality*, SIAM J. Appl. Math., 81(4):1717–1741, 2020. 1

[39] L. Preziosi, G. Toscani, and M. Zanella, *Control of tumor growth distributions through kinetic methods*, J. Theor. Biol., 514:110579, 2021. 1

[40] M. Torregrossa and G. Toscani, *On a Fokker-Planck equation for wealth distribution*, Kinet. Relat. Models, 11(2):337–355, 2018. 1

[41] G. Toscani, A. Tosin, and M. Zanella, *Kinetic modelling of multiple interactions in socio-economic systems*, Netw. Heterog. Media, 15(3):519–542, 2020. 2.1

[42] T. Trimborn, L. Pareschi, and M. Frank, *Portfolio optimization and model predictive control: A kinetic approach*, Discrete Contin. Dyn. Syst. Ser. B, 24(11):6209–6238, 2019. 2.1

[43] S. Hoya White, A.Martin del Rey, and G. Rodríguez Sánchez, *Modeling epidemics using cellular automata*, Appl. Math. Comput., 186(1):193–202, 2007. 1